

**CHEMISTRY AND BIOLOGY OF SALINOMYCIN AND ITS ANALOGUES**DOI: <http://dx.medra.org/10.17374/targets.2016.19.177>**Anna Piperno,<sup>a,\*</sup> Agostino Marrazzo,<sup>b</sup> Angela Scala<sup>a</sup> and Antonio Rescifina<sup>b,\*</sup>**<sup>a</sup>*Department of Chemical, Biological, Pharmaceutical and Environmental Sciences,  
University of Messina, Viale Ferdinando Stagno D'Alcontres 31, 98166 Messina, Italy*<sup>b</sup>*Department of Drug Sciences, University of Catania, Viale Andrea Doria 6, 95125 Catania, Italy  
(e-mail: arescifina@unict.it)*

**Abstract.** Natural carboxylic polyether ionophores such as salinomycin, monensin, and lasalocid have been objects of great interest because of their antibacterial, antifungal, antiparasitic, and antiviral activities. Recently, it has been found that polyether ionophores might be also important chemotherapeutic agents in the treatment of cancer. These compounds have shown potent activity against the proliferation of various cancer cells, including those that display multidrug resistance (MDR), and cancer stem cells (CSCs). This chapter deals with the structure, synthesis, chemical and biological properties of salinomycin and its derivatives.

**Contents**

1. Introduction
  2. Synthesis of salinomycin
    - 2.1. Total synthesis
    - 2.2. Enhanced partial syntheses
      - 2.2.1. Syntheses of the western hemisphere
      - 2.2.2. Syntheses of the eastern hemisphere
  3. Salinomycin derivatives
    - 3.1. Modification of the carboxyl group
      - 3.1.1. Amides
      - 3.1.2. Esters
    - 3.2. Modification of the hydroxyl groups
      - 3.2.1. Conjugates (*O*-acylates at C<sub>9</sub>, C<sub>20</sub>, and C<sub>28</sub>)
    - 3.3. Reduction and oxidation
      - 3.3.1. Synthesis of 20-deoxy salinomycin (SY1) and 18,19-dihydro SY1
    - 3.4. Salinomycin hybrid compounds
    - 3.5. Metal complexes of salinomycin
  4. Ionophore properties
  5. Mechanism of action
  6. Structure-activity relationships
  7. Salinomycin as a drug for targeting human cancer stem cells
  8. Conclusions
- References

## 1. Introduction

Polyether ionophores represent a very large and important group of naturally occurring compounds produced by *Streptomyces spp.* Increased interest in compounds of this type has been observed in recent years. There are over 120 naturally occurring ionophores known so far.<sup>1</sup> Major commercial use of ionophores is to control coccidiosis. They are also used as growth promoters in ruminants. These compounds specifically target the ruminal bacteria populations and their use permits increasing production efficiency of the livestock. In 2003, the antimicrobials most commonly used in beef cattle production were ionophores.<sup>2</sup> Polyether skeletons of the pseudocyclic structure of polyether ionophores are able to form complexes with metal cations and facilitate their transport across cellular membranes. It has been shown that the chemical modification of polyether antibiotics can change the ability and the selectivity of metal cations binding and modifying the mechanism of cation transport, thereby leading to new antibacterial and anticancer active compounds. Moreover, ionophores can also be used in the production of ion-selective electrodes.<sup>3,4</sup>

All the aforementioned applications of ionophores are closely related to their structure and ability to form complexes with metal cations (host-guest complexes) and transport these complexes across lipid bilayers and cell membranes.

Salinomycin (SAL, **1**) is a polyether antibiotic isolated from the culture broth of *Streptomyces albus* (strain no. 80614) by Miyazaki and colleagues from the research division of Kaken Chemicals Co., Ltd., Tokyo, Japan, during the course of a screening program for new antibiotics.<sup>5</sup> The production of SAL was carried out by tank fermentation, filtration of culture broth, purification by column chromatography on alumina or silica gel and crystallization. By this isolation procedure, SAL was obtained as a colorless prism of the sodium salt.

Structurally, the SAL molecular architecture is dominated by the presence of 18 chiral centers embedded in a poly-oxygenated backbone, which encompass two substituted tetrahydropyrans (A and E rings, Figure 1) and a complex tricyclic bis-spiroacetal system (B-D rings, Figure 1), and the IUPAC name is (2*R*)-2-[(2*R*,5*S*,6*R*)-6-[(2*S*,3*S*,4*S*,6*R*)-6-[(2*S*,5*S*,7*R*,9*S*,10*S*,12*R*,15*R*)-2-[(2*R*,5*R*,6*S*)-5-ethyl-5-hydroxy-6-methyltetrahydro-2*H*-pyran-2-yl]-15-hydroxy-2,10,12-trimethyl-1,6,8-trioxadispiro[4.1.5.3]pentadec-13-en-9-yl]-3-hydroxy-4-methyl-5-oxooctan-2-yl]-5-methyltetrahydro-2*H*-pyran-2-yl]butanoic acid.

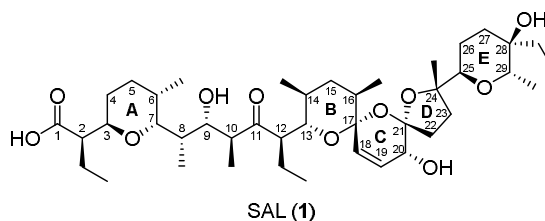


**Figure 1.** Structure and backbone numeration of salinomycin.

Full characterization of SAL has been endorsed by X-ray crystallographic analysis on the SAL *p*-iodophenacyl ester,<sup>6</sup> and successively, in solution, by extensive NMR studies in CDCl<sub>3</sub>, DMSO-d<sub>6</sub>, and acetonitrile-d<sub>3</sub> solvents.<sup>7-9</sup>

SAL is a weakly acidic compound ( $pK_a$  6.4 in DMF) with molecular formula  $C_{42}H_{70}O_{11}$ , mass of 751 Da, melting point of 112.5-113.0 °C, UV absorption at 285 nm, and  $[\alpha]_D^{25} = -63^\circ$ . SAL free acid is insoluble in water, and soluble in lower alcohols, acetone, ethyl acetate, chloroform, ether, petroleum ether and hexane.<sup>5</sup>

SAL was obtained from its commercially available sodium salt according to the following method: the SAL sodium salt was dissolved in  $CH_2Cl_2$  (DCM) and vigorously stirred for 12 h with aqueous  $H_2SO_4$ . The organic phase was washed with water, until neutrality, and evaporated under reduced pressure to obtain an oily residue. The most effective conversion was observed at pH 2.0.<sup>10</sup>

Using more concentrated sulphuric acid solutions (pH 1.0), an isomer of SAL was isolated as a result of a rearrangement. The proposed mechanism of the rearrangement starts with the protonation of  $O_{13}$  and then involves the tertiary carbocation stabilized by the oxygen atom  $O_{17}$  and ends with a nucleophilic attack of the electron pair from  $O_{20}$  on  $C_{24}$  which is engaged in the bond closing the new ten-membered ring. The new isomer was fully characterized by 2D NMR, NOESY, and MALDI-TOF, and its properties were studied by semiempirical (PM5) and DFT (B3LYP) methods.<sup>10</sup>

Additionally, HPLC-MS studies have indicated that SAL degraded when stored as water/methanol solution at room temperature, by the opening of the spiro rings and the concomitant formation of a furan moiety.<sup>7</sup>

The use of SAL in veterinary medicine can be traced back to the early eighties as a broad-spectrum antimicrobial agent with activity against gram-positive bacteria including *Bacillus subtilis*, *Staphylococcus aureus*, *Micrococcus flavus*, *Sarcina lutea* and *Mycobacterium spp.*, some filamentous fungi, *Plasmodium falciparum* and *Eimeria spp.*, the latter constitute protozoan parasites responsible for the coccidiosis, an intestinal plasmodium infection typical of poultry and rabbits. No activity was observed in gram-negative bacteria and yeast. The anticoccidial estimation of SAL was carried out with chickens infected with *Eimeria tenella* (Coccidia, Sporozoa) oocysts, resulting effective in reducing the mortality of chickens from coccidiosis.<sup>5</sup> Thus, a patent has been issued for the use of SAL to prevent coccidiosis in poultry,<sup>11</sup> and up to now SAL is one of the most widely used ionophoric coccidiostats in poultry in the USA, to control or prevent coccidian parasite infestation, and it is also used as growth promoter for ruminants and pigs to improve nutrient absorption and feed efficiency.<sup>12</sup>

As an antimicrobial drug, SAL acts as a cation ionophore interfering with ions exchanges at the cell membranes, including cytoplasmic and mitochondrial membranes, of the target organisms. In particular, ionophore antimicrobials are able to form lipid-soluble complexes with cations (especially  $K^+$ ) that can cross the membranes by passive diffusion. Such ions fluxes, independent from ions channels and membranes potential, disrupt the osmotic balance, ultimately resulting in cell death.<sup>13,14</sup>

Especial attention has been paid to SAL since 2009, when it was announced by Gupta and colleagues that, in a sophisticated high-throughput screening of 16000 chemicals, SAL resulted nearly 100-fold more effective towards the breast cancer stem cells (CSCs) than paclitaxel (Taxol), the commonly used anti-breast cancer drug.<sup>15</sup> Based on these findings, SAL was tested on a small group of patients with invasive carcinoma of the head, neck, breast and ovary. Intravenous administration of SAL (200-250  $\mu g/kg$ ) every second day for three weeks resulted in partial regression of tumor metastasis over an extended period of time. Acute side effects were rare and the serious long-term adverse side effects observed with conventional chemotherapeutic drugs were not registered.<sup>16</sup>

Moreover, the selective cytotoxic effect of SAL on CSCs was also detected in osteosarcoma *in vitro* and *in vivo*. Additionally, SAL also sensitizes these CSCs to conventional chemotherapeutic drugs including methotrexate, adriamycin, and cisplatin.<sup>17</sup>

Recently, Boehmerie and Endres demonstrated that one important caveat for the potential clinical application of SAL is its severe neural and muscular toxicity, mediated by elevated cytosolic Na<sup>+</sup> concentrations, which in turn cause an increase of Ca<sup>2+</sup>, followed by activation of the protease calpain and subsequent caspase-dependent apoptotic cell death.<sup>18</sup> Several reports published in the last three decades reported that accidental ingestion of SAL results in severe toxicity in mammals, such as horses, cats, dogs, pigs, as well as human.<sup>19-23</sup>

Risk assessment data recently published by the European Food Safety Authority declare an acceptable daily intake (ADI) of 5 µg/kg SAL for humans because daily intake of more than 500 µg/kg SAL by dogs leads to neurotoxic effects such as myelin loss and axonal degeneration.<sup>24</sup>

## 2. Synthesis of salinomycin

Since SAL discovery, but especially after the evidence of its potent biological activity, the synthetic challenges raised by such intricate and densely functionalized structure have stimulated researchers to devise efficient and strategic methodologies to its laboratorial organic synthesis. These efforts have culminated in three total syntheses and new approaches to both the tetrahydropyran ring flanked by an  $\alpha$ -alkyl acetic acid and a polyketide chain (western hemisphere) and the spiroacetal core (eastern hemisphere).

### 2.1. Total synthesis

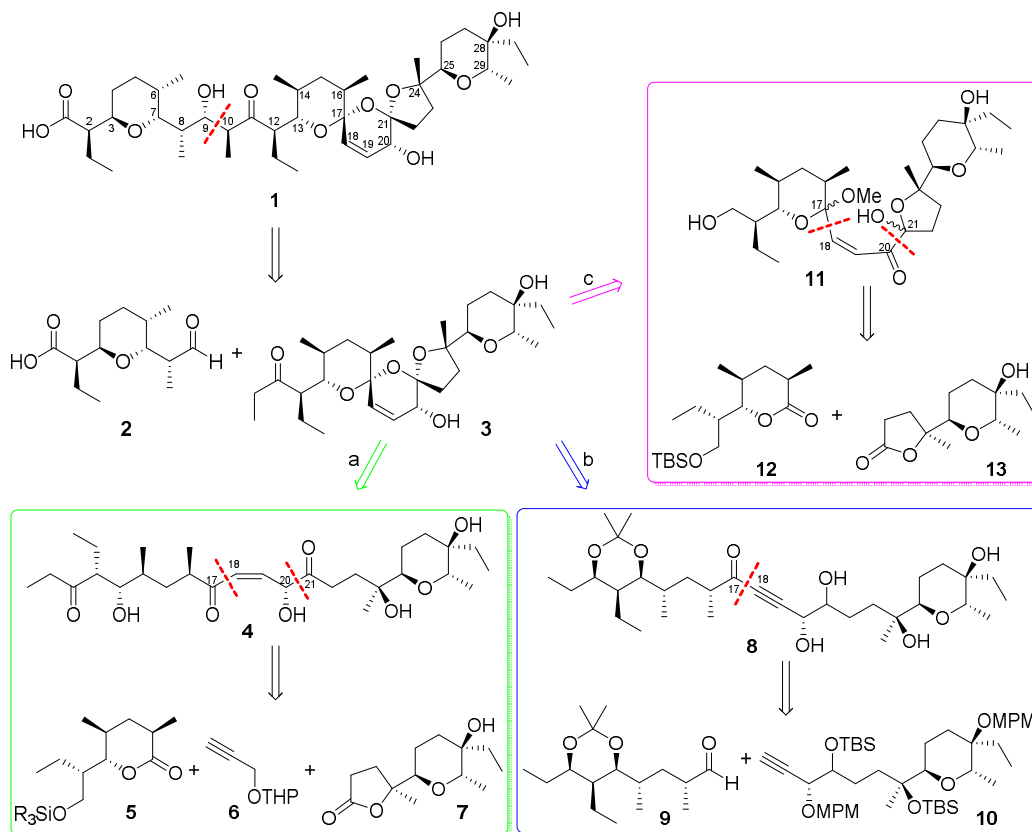
The three total syntheses, developed by Kishi (1981),<sup>25</sup> Yonemitsu (1989),<sup>26-29</sup> and Kocienski (1994),<sup>30-32</sup> share the first step in their retrosynthetic pathway that is the disconnection of the C<sub>9</sub>-C<sub>10</sub> bond (Scheme 1), equivalent to a stereoselective crossed aldol condensation in the synthetic direction. The two fragments afforded by this disconnection, tetrahydropyran **2** and bis-spiroacetal **3**, are conventionally termed the left and right-hand fragments, respectively.

Following route a (Scheme 1) Kishi envisaged in fragment **4** the potential precursor of **3** and proceeded disconnecting it at C<sub>17</sub>-C<sub>18</sub> and C<sub>20</sub>-C<sub>21</sub> bonds to individuate further three subunits, **5-7**, as starting points. Kishi's synthesis was noteworthy for two reasons: (a) it amplified and extended a general strategy for polyketide synthesis based on directed olefin epoxidation and regioselective oxirane cleavage and (b) it grappled for the first time with the thorny issue of spiroacetalisation stereochemistry in the complex dispiroacetal core.

A chiral pool strategy was used in the second synthesis of SAL by the Yonemitsu group to construct the entire skeleton from three cheap precursors: D-glucose, D-mannitol and ethyl (*S*)-lactate. So, following path b (Scheme 1) the alkyne **8** was identified as the direct generator of **3** and was disconnected at C<sub>17</sub>-C<sub>18</sub> bond to furnish other two subunits, **9** and **10**. These fragments have to be synthesized from sugars. An enduring contribution of this group to organic synthesis was the development of the *p*-methoxybenzyl and 3,4-dimethoxybenzyl ether as protecting groups for hydroxyl functions.

In the most recent total synthesis, following path c (Scheme 1), Kocienski idealized the opening of **3**, at C<sub>17</sub> acetal position, to afford the allenol ether **11**, which was further disconnected at the C<sub>17</sub>-C<sub>18</sub> and C<sub>20</sub>-

$C_{21}$  bonds to reveal the two new lactones **12** and **13**. The approach of Kocienski has the following features: (a) the alkylation of an  $\eta^3$ -molybdenum cationic complex by an  $\alpha$ -alkoxyalkyl cuprate to append a stereogenic center to an oxane ring; (b) the use of a spirocyclic molybdenum carbene complex as a precursor to a furan; (c) the asymmetric oxidation of a 1,5-diene to create four stereogenic centers in a single step; (d) two different approaches to the 1,6,8-trioxadispiro-[4.1.5.3]pentadec-13-ene ring system, one based on Achmatowicz's furan oxidation and the other on the acylation-protonation of a metallated allenol ether intermediate.



**Scheme 1.** a) Kishi route; b) Yonemitsu route; c) Kocienski route.

These three approaches have been extensively reviewed by Brimble and Farès,<sup>33</sup> and by Faul and Huff,<sup>34</sup> therefore, here we report only their stereochemical inventory (Table 1).

## 2.2. Enhanced partial syntheses

Due to the success and the renewed interest in SAL, many researchers have tried to optimize the yields and the stereochemistry outcome overcoming the critical points emerged in the first three total syntheses.

**Table 1.** Stereochemical inventory for the total synthesis of SAL.

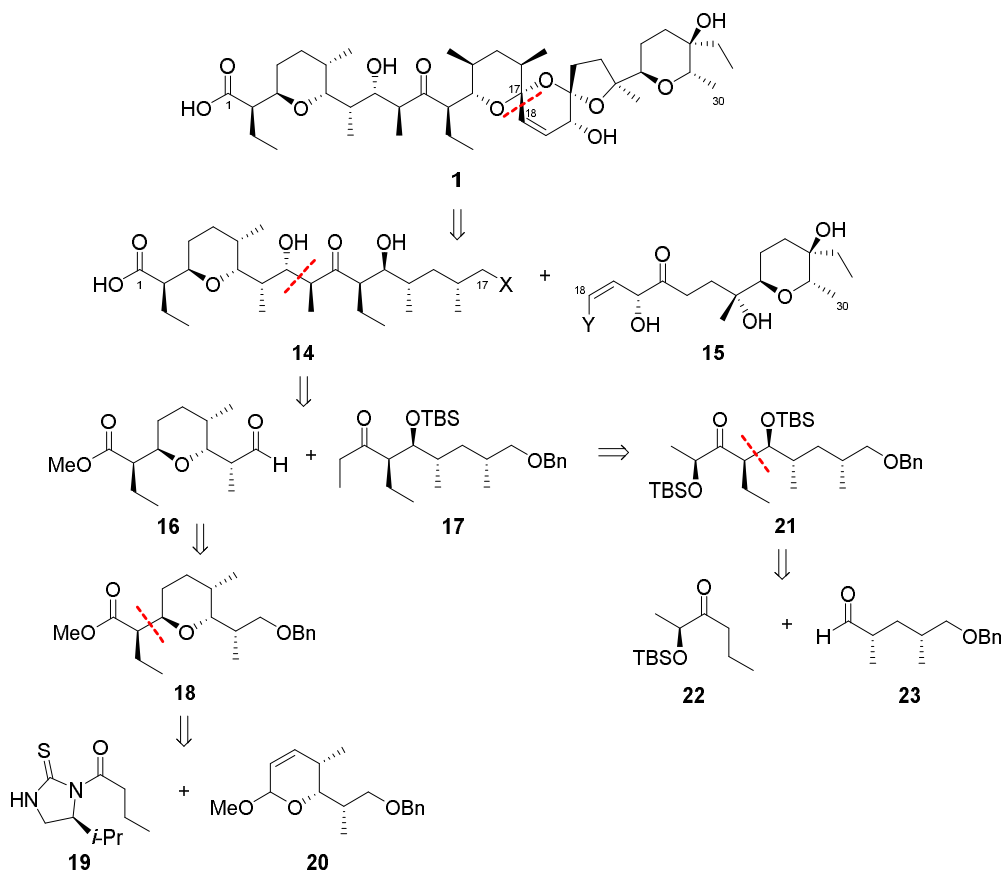
carbon	Kishi		Yonemitsu		Kocienski	
	method	reaction/source	method	reaction/source	method	reaction/source
C <sub>2</sub>	A-1,3	epoxidation	chiral pool	D-glucose	A-1,3	Sharpless AE
C <sub>3</sub>	A-1,3	epoxidation	Cram-chelate	Grignard addn	A-1,3	Sharpless AE
C <sub>6</sub>	A-1,3	epoxidation	chiral pool	D-glucose	thermodynamic	THP formation
C <sub>7</sub>	A-1,3	Sharpless AE	chiral pool	D-glucose	radical anomeric effect	lithium 4,4'-di-tert-butylbiphenylide
C <sub>8</sub>	A-1,3	Sharpless AE	chiral pool	D-glucose	chiral pool	$\eta^3$ -allyl Mo complex
C <sub>9</sub>	Cram addn	aldol/Mg enolate	Cram addn	aldol/Mg enolate	Cram addn	aldol/Mg enolate
C <sub>10</sub>	Cram addn	aldol/Mg enolate	Cram addn	aldol/Mg enolate	Cram addn	aldol/Mg enolate
C <sub>12</sub>	A-1,3	epoxidation	chiral pool	D-glucose	A-1,3	aldol/oxazolidinethione
C <sub>13</sub>	A-1,3	epoxidation	chiral pool	D-glucose	A-1,3	aldol/oxazolidinethione
C <sub>14</sub>	chiral pool	(+)-3-hydroxypropanoic acid	chiral pool	D-glucose	resolution	$\alpha$ -methylbenzylamine
C <sub>16</sub>	A-1,3	epoxidation	cyclic stereocontrol	hydrogenation	resolution	$\alpha$ -methylbenzylamine
C <sub>17</sub>	thermodynamic	equilibration	thermodynamic	equilibration	thermodynamic	equilibration
C <sub>20</sub>	nonselective	alkyl lithium addn	chiral pool	D-glucose	Cram-chelate	hydride/Mitsunobu
C <sub>21</sub>	thermodynamic	equilibration	thermodynamic	equilibration	thermodynamic	equilibration
C <sub>24</sub>	Cram-chelate	Grignard addn	Cram-chelate	organolithium addn	KMnO <sub>4</sub> oxidative cyclization	(2 <i>S</i> )-bornane-10,2-sultam
C <sub>25</sub>	directed reduction	hydride addn	chiral pool	D-mannitol	KMnO <sub>4</sub> oxidative cyclization	(2 <i>S</i> )-bornane-10,2-sultam
C <sub>28</sub>	A-1,3	epoxidation	Cram-chelate	Grignard addn	KMnO <sub>4</sub> oxidative cyclization	(2 <i>S</i> )-bornane-10,2-sultam
C <sub>29</sub>	A-1,3	epoxidation	chiral pool	( <i>S</i> )-lactate	KMnO <sub>4</sub> oxidative cyclization	(2 <i>S</i> )-bornane-10,2-sultam

### 2.2.1. Syntheses of the western hemisphere

Urpi (2006)<sup>35</sup> and Yadav (2014)<sup>36</sup> reported two enhanced and intriguing syntheses of the western hemisphere. Urpi used a convergent and module-based strategy relayed on highly stereoselective *C*-glycosylation and substrate-controlled aldol processes, whereas Yadav employed a desymmetrization

approach and an intramolecular oxetane opening reaction with *O*-nucleophile to obtain the tetrahydropyran skeleton.

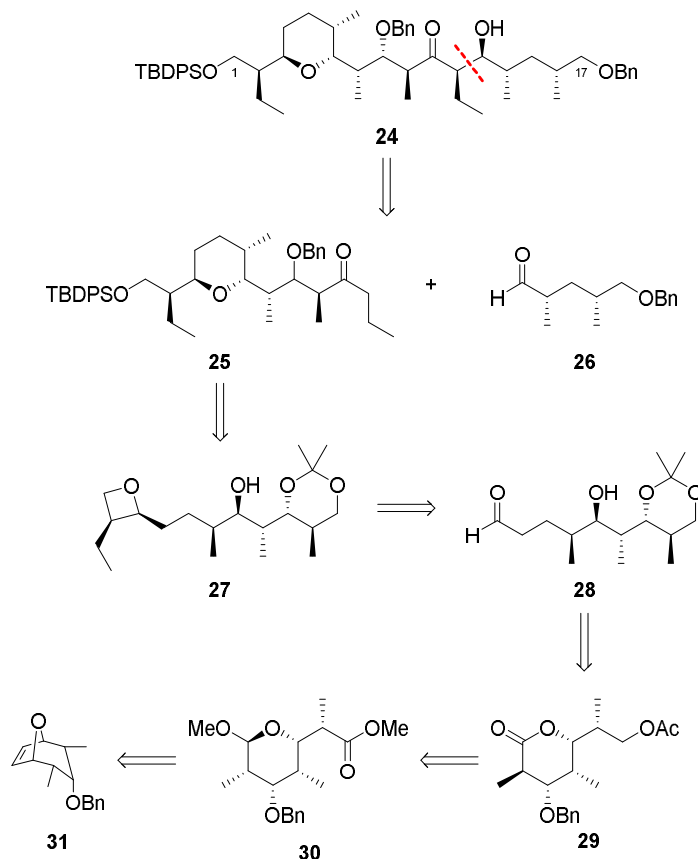
As outlined in Scheme 2, Urpi's approach consists in the strategic disconnection of the C<sub>17</sub>-C<sub>18</sub> bond of SAL that splits it into two halves of similar size and complexity, the western **14** and eastern **15** hemispheres. Further elaboration of the western hemisphere revealed the need to protect the acidic moiety as methyl ester and the hydroxyl at C<sub>13</sub> as *tert*-butyldimethylsilyl ether. So, the construction of fragment **14** can be outlined in the following three steps: (i) a double asymmetric *anti* aldol reaction of ketone **17** and aldehyde **16**, obtained by C<sub>9</sub>-C<sub>10</sub> bond disconnection; (ii) a Lewis acid mediated *C*-glycosidation involving titanium enolate from (*S*)-*N*-substituted-1,3-thiazolidine-2-thione **19** and glycal **20**; (iii) a double asymmetric *syn* aldol reaction arising from  $\alpha$ -hydroxy ketone **22** and aldehyde **23**. Hemisphere **14** has been synthesized in twelve steps with an overall yield of 11.4%.



**Scheme 2.** Disconnection approach for the synthesis of SAL's western hemisphere according to Urpi protocol.

Respect to Urpi, Yadav used both a different protection, identifying fragment **24** as the western

hemisphere precursor and a different point of disconnection, i.e. C<sub>12</sub>-C<sub>13</sub> bond (Scheme 3). The synthesis of the fragment **24** was effectuated utilizing a substrate controlled *syn*-aldol reaction following Urpi's protocol<sup>37</sup> wherein the reaction occurs *via* the *Z*-enolate of the benzylated  $\beta$ -hydroxy ketone **25** that adds onto the aldehyde **26** through a chelating chair-like transition state. The functionalized *trans*-tetrahydropyran ring present in **25** was envisioned to be constructed *via* an acid catalyzed intramolecular regioselective oxetane ring-opening reaction in an *exo*-cyclization fashion followed by sequential functional group manipulations to further extend the chain. The oxetane ring in **27** was synthesized by an Evans *syn*-aldol reaction of aldehyde **28** which in turn was obtained from lactone **29**. This last was easily accessed from acetal **30** in five steps, whereas **30** was obtained by a desymmetrization approach from the symmetric bicyclic olefin **31**.



**Scheme 3.** Disconnection approach for the synthesis of SAL's western hemisphere according to Yadav protocol.

The most demanding step was the intramolecular oxetane ring-opening process that required an accurate optimization of the reaction conditions to arrive at the correct regio- and stereo-chemical outcome.

The synthesis involved twenty-four steps, starting from **30**, with a 10.2% overall yield.

### 2.2.2. Syntheses of the eastern hemisphere

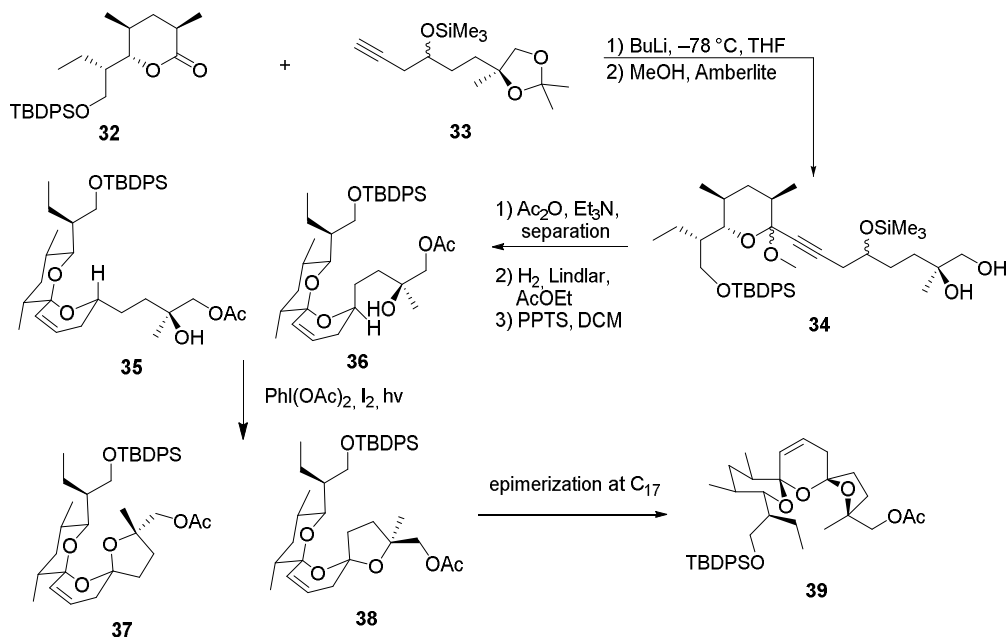
The real issue in the synthesis of the eastern hemisphere is the construction of the tricyclic bis-spiroacetal system. The traditional approach to these structures, since 1988, was the stepwise construction of a linear precursor followed by an acid catalyzed ketalisation-cyclization event, or several domino events, and many syntheses have been accomplished in this manner.<sup>33</sup> These methods rely on the control of stereochemistry at the anomeric center being dictated by the relative thermodynamic stability of the different isomers formed using an acid-catalyzed spiroacetalisation step. The major isomer produced in this case is that which has the maximum number of anomeric effects with minimum steric interactions. When these two factors work in opposite directions lower stereoselectivity is observed. In tricyclic bis-spiroacetal systems the balance between these factors needs careful consideration when predicting the outcome of the spiroacetalisation step as the small differences in energy and interconversion barriers often lead to the formation of a range of isomeric structures.

So, the new challenge was the design of alternative methods to make bis-spiroacetals that avoid some of the efficiency pitfalls of the more traditional chemistry; amongst these new ideas, are noteworthy those of Brimble<sup>38,39</sup> and Vassilikogiannakis.<sup>40-42</sup> The Brimble's approach consisted of a kinetically controlled oxidative radical cyclization *via* intramolecular hydrogen abstraction, that also provides a convenient method to access the thermodynamically less stable isomers, whereas the Vassilikogiannakis's one was based upon the use of furan oxidations by singlet oxygen.

In the first case, assembly of the bis-spiroacetal core of SAL was effected starting from lactone **32** and acetylene **33** (Scheme 4). The addition of the lithium acetylide derived from acetylene **33** to lactone **32** followed by treatment of the intermediate lactol with methanol and Amberlite IR 118 resin effected hydrolysis of the acetonide group and formation of more stable methyl acetals **34** as a mixture of diastereomers that were separated after the protection of the primary hydroxyl group. Partial hydrogenation of the acetylated alkynes **34** to a *cis*-olefin followed by acid catalyzed cyclization resulted in a 1:1 mixture of spiroacetals **35** and **36** that were inseparable by flash chromatography. This initial spirocyclization is carried out under thermodynamically controlled conditions such that the most stable configuration is afforded at the newly formed spiro center owing to maximum stabilization by the anomeric effect. Therefore, the two isomeric spiroacetals **35** and **36** differ only in the position of the side chain. When these spiroacetals were treated with iodobenzene diacetate and iodine afforded a 1:1.7 mixture of tricyclic bis-spiroacetals **37** and **38**. The preference for *trans* bis-spiroacetal **38** in this cyclization reaction was explained by the proposed mechanism wherein both diastereomeric precursors **35** and **36** form the same carbocation intermediate (derived from the corresponding free radical), that, successively, is predominantly trapped from the least hindered  $\alpha$ -face.

The minor bis-spiroacetal **37** isolated from this oxidative cyclization has the 17-*epi*-21-*epi*SAL stereochemistry whereas the major isomer **38** has the 17-*epi*SAL stereochemistry. Given that it is well established that long-range hydrogen bonding in the final molecule can dramatically alter the position of the bis-spiroacetal equilibrium, it was envisaged that thermodynamically controlled cyclization after the whole carbon skeleton of the natural product has been assembled, will allow convergence of the bis-spiroacetal

stereochemistry to that depicted in *cis* isomer **39**, due to an epimerization at the allylic spiro center.



**Scheme 4.** Synthesis of the tricyclic bis-spiroacetal core of SAL by kinetically controlled oxidative radical cyclization *via* intramolecular hydrogen abstraction.

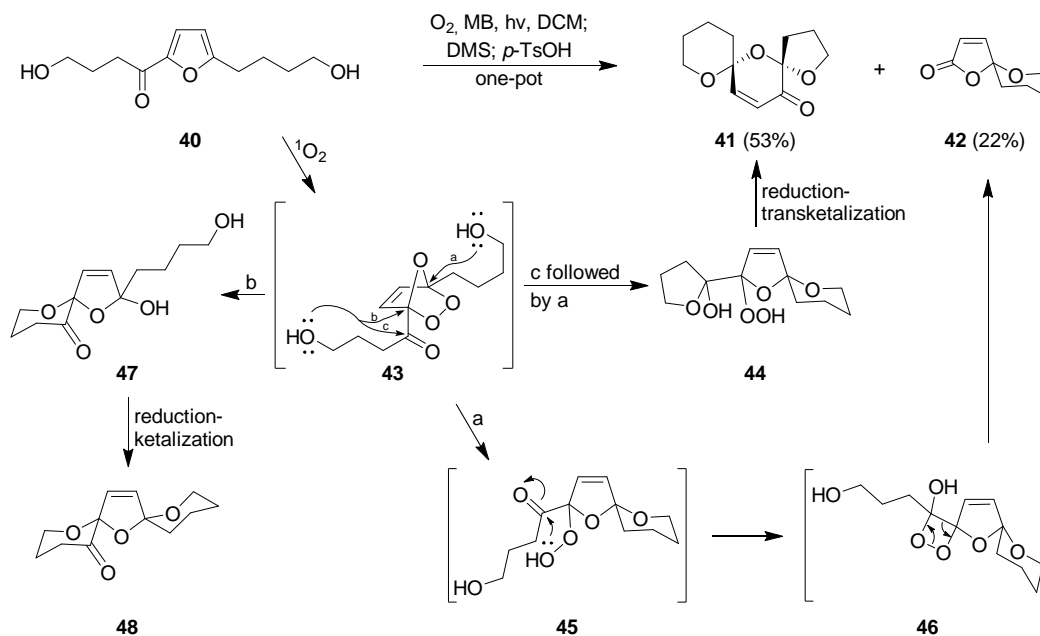
The approach of Vassilikogiannakis was inspired by the use of furan oxidations as a starting point for the synthesis of bis-spiroacetals; however, application of this approach was frequently limited to simple substrates in response to the harsh/non-selective oxidants employed (e.g. Br<sub>2</sub>, NBS, or electrochemical oxidation). A noteworthy exception to this simple substrate-limitation is to be found within the investigations that culminated in several elegant total syntheses of SAL by Kocienski's group (*vide supra*).

So, Vassilikogiannakis had the idea to develop a synthetic procedure based on tandem and cascade reaction sequences mediated by singlet oxygen (<sup>1</sup>O<sub>2</sub>) as a clean and selective oxidant to synthesize the tricyclic bis-spiroacetal key motif.

The advantages of using a singlet oxygen based approach are multiple: first, <sup>1</sup>O<sub>2</sub> is highly selective and requires little by the way of protection for other functional groups, and second, the whole transformation is easily performed in one pot with all the inherent advantages of efficiency that such an approach holds; furthermore, these reactions, in principle, could also be undertaken in water using the natural sensitizer, spirulina, and no reductant in a highly sustainable set of protocols.

The desired [6,6,5]-bis-spiroacetal motif was accessed from a substrate bearing a furfuryl carbonyl moiety, through a one-pot cascade reaction sequence, despite the fact that two competing fragmentation processes were also uncovered (Scheme 5).<sup>42</sup> The kinetics of these reactions worked favorably, and, when diol **40** was treated to the established <sup>1</sup>O<sub>2</sub> reaction conditions (10<sup>-4</sup> M methylene blue as sensitizer, oxygen

bubbling through a cooled solution, and visible spectrum light irradiation for 5 min), followed by dimethyl sulphure- (DMS) mediated reduction and subsequent addition of mild acid (*p*-TsOH) to assist the final cyclization, the formation of SAL-type [5,6,6]-bis-spiroacetal **41** as the major product (53%) was observed. The product of an unwanted fragmentation, spiro lactone **42**, was also observed but in a much reduced percentage (22%) compared with the earlier model studies. A simplified explanation of the outcome is as follows: from diol **40**, an ozonide adduct **43** is initially formed that may suffer any one of three different fates (see pathways a, b, and c, Scheme 5).



**Scheme 5.** Synthesis of the tricyclic bis-spiroacetal core of SAL by tandem and cascade reaction sequences mediated by singlet oxygen.

The product distribution would suggest that pathway *c* attack is the fastest (thus, suppressing pathway *b* altogether) of these alternatives, but that pathway *a* does still compete to a small extent. In this way, the reaction is funneled down two distinct avenues; first, the dominant pathway converts the ozonide **43** into spirocycle **44**, through sequential pathway *c* and *a* attacks in quick succession, that is then reduced (by DMS) and subject to transketalization (upon addition of TsOH) to furnish the desired [5,6,6]-bis-spiroacetal **41**. The minor pathway sees a type *a* attack on the ozonide **43** to yield spirocycle **45**, which then rearranges to **46** that successively fragments to give spiro lactone **42**. Thus, a model for the [5,6,6]-bis-spiroacetal motif of salinomycin had been synthesized in one pot from a readily accessible acyl furan. The adjustments of this method to effectively produce eastern hemisphere of SAL are in progress.

### 3. Salinomycin derivatives

Semi synthesis of analogs through selective chemical modification of SAL constitutes an attractive

avenue for identifying compounds with improved selectivity against CSCs and for advancing the structural understanding of the mechanism of action of SAL. Several investigations of semi-synthetic derivatives of SAL have shown that chemical modifications can change the ability and selectivity of binding to metal cations, and lead to new active compounds that can be hopefully less toxic for humans. The modifications were mainly focused on the oxygen functions such as carboxylic acid, hydroxyl, and ketone groups which are involved in the ion binding to form cation-complex.

### 3.1. Modification of the carboxyl group

#### 3.1.1. Amides

The synthesis of amides is one of the most fundamental methods in organic chemistry used to obtain natural and synthetically useful compounds.<sup>43,44</sup> Several amidation procedures require rigorous conditions, for example the synthesis from acyl chlorides. However, since SAL is very sensitive to acidic conditions and heating, mild amidation reaction conditions must be chosen. The first direct and practical approach to the synthesis of amide derivatives of SAL (**49–90**) was described in 2012 by Huczynski and co-workers,<sup>45</sup> using DCC (*N,N'*-dicyclohexylcarbodiimide) as a coupling agent and HOBt (1-hydroxybenzotriazole) as an activator (Scheme 6). The reaction was carried out at room temperature on SAL carboxylic acid, preventively obtained from SAL sodium salt by extraction with H<sub>2</sub>SO<sub>4</sub> (pH 1.5) in DCM (dichloromethane). SAL sodium salt was in turn isolated from premix (SACOX<sup>®</sup>, commercially veterinary feed additive) which contains about 12% of SAL. The key advantages of this method are good yields, easy work-up and purification of the products by dry column vacuum chromatography and crystallization.<sup>46</sup>

This simple and efficient one-pot protocol was applied to the commercially available aliphatic and aromatic primary amines (Scheme 6, a),<sup>45,47,48</sup> to the aliphatic secondary amines (Scheme 6, b),<sup>49</sup> to the mono-substituted benzyl amines with fluorine, chlorine and bromine atoms as well as nitro group in ortho, meta and para positions (Scheme 6, c),<sup>50</sup> and, finally, to the methyl esters of selected naturally occurring amino acids (Scheme 6, d).<sup>51</sup>

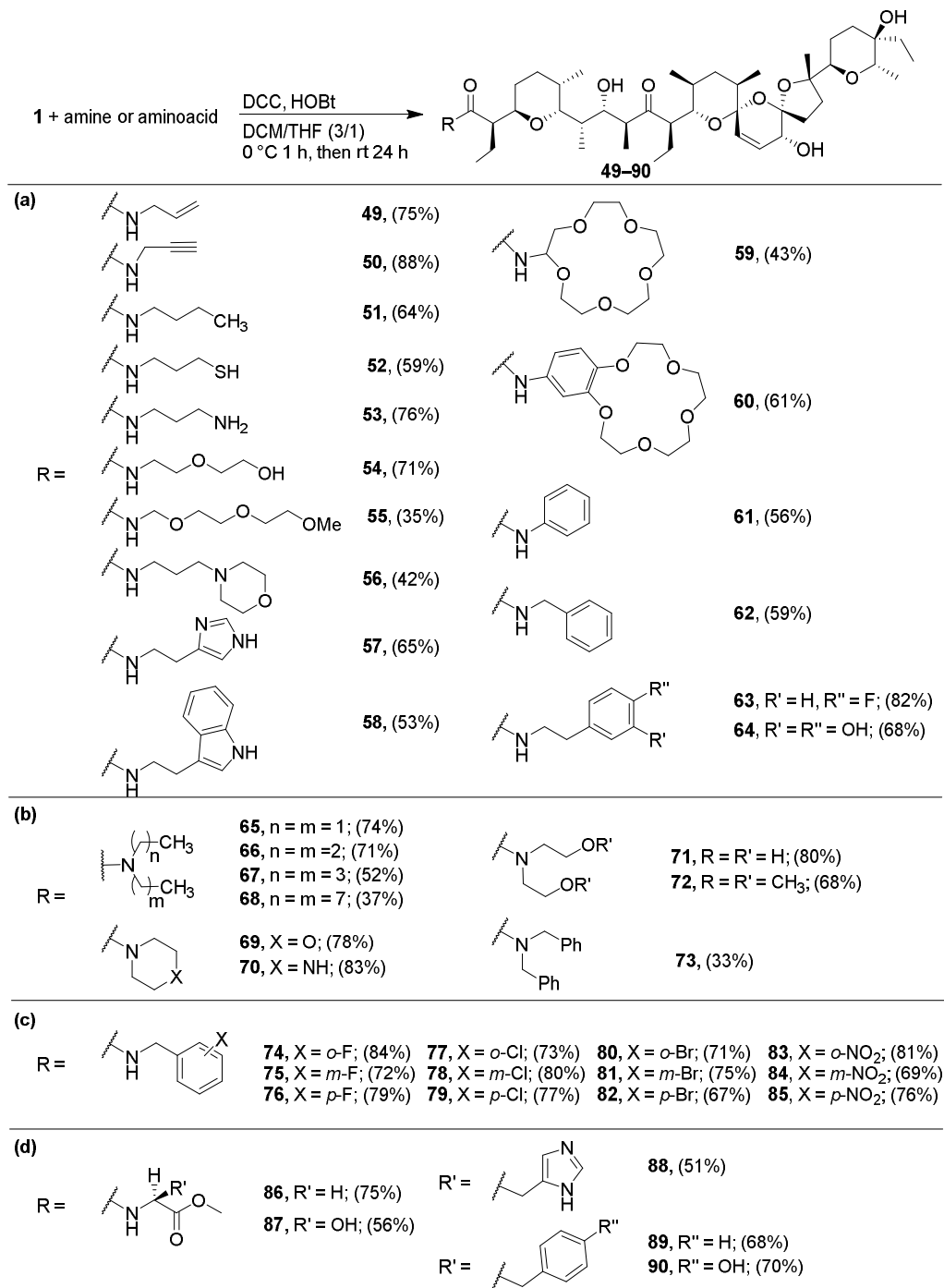
In the reaction between SAL and 1-naphthylamine the expected amide product was not observed, rather an unexpected stable benzotriazole ester of SAL (**91**, SAL-HOBT) has been isolated and structurally characterized as an intermediate product of the amidation reaction (Figure 2).<sup>52</sup>

Since it is generally believed that dimers of biologically active compounds, such as antibiotics, can show enhanced biological activity with respect to that of the single ligand, in order to check the effects of linker length and its flexibility on the biological activity of SAL, three symmetrical dimers were prepared coupling two SAL molecules with different diamines (1,4-butanediamine, *p*-phenylenediamine, 4,4'-diaminobiphenyl; Figure 3).<sup>47</sup> Only compound **94** showed activity against Gram-positive bacteria.

#### 3.1.2. Esters

Most procedures of esterification require rather harsh conditions such as the presence of strong acids, bases or other catalysts and high temperatures. Nevertheless, mild reaction conditions for SAL esterification have to be adopted to overcome the sensitivity of SAL to acidic conditions and heating.

In a pioneering work the methyl and the *p*-bromophenacyl esters of SAL were prepared by reacting SAL with an excess of ethereal diazomethane and with *p*-bromophenacyl bromide in ethanol, respectively.<sup>53</sup>



Scheme 6. Amide derivatives of SAL.

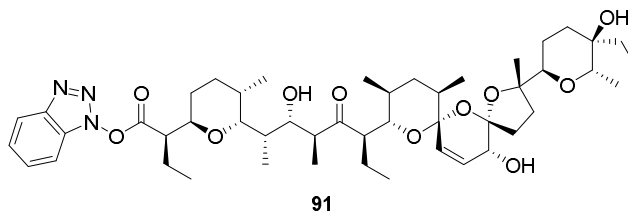


**Figure 2.** SAL-HOBT.

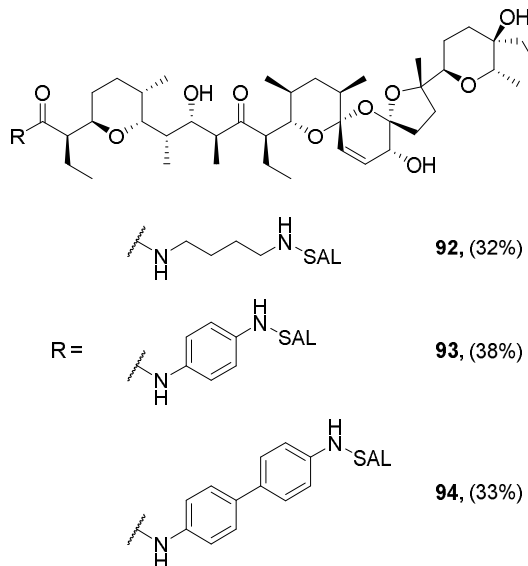
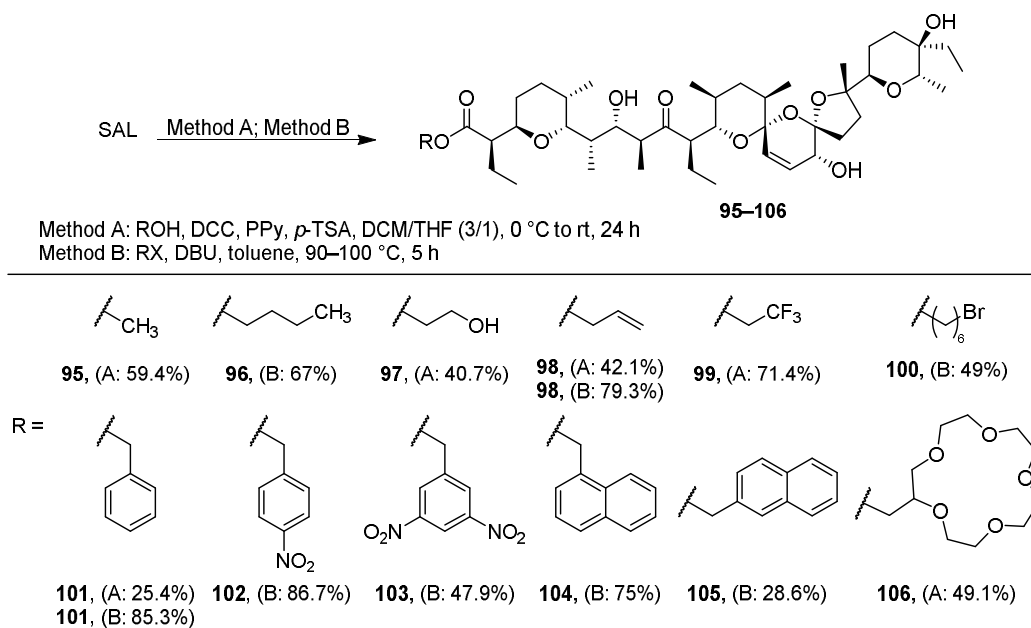


**Figure 3.** Symmetrical dimers of SAL.

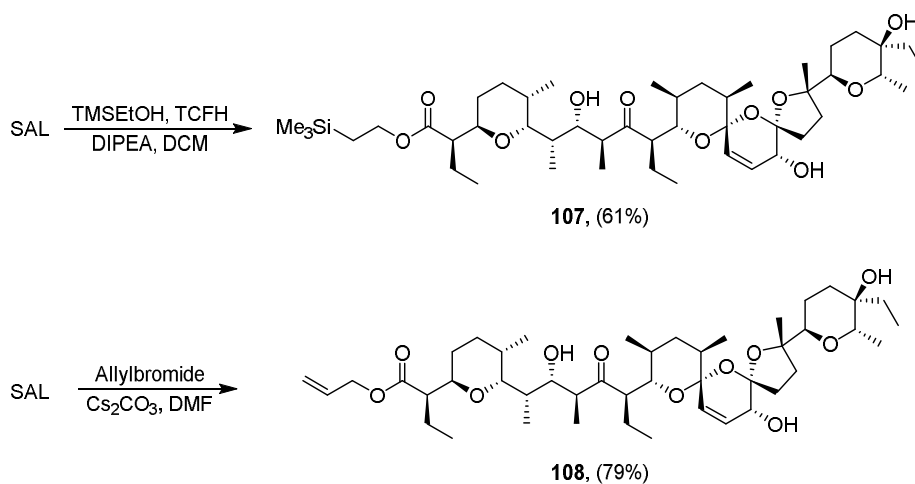
Recently, valuable methods for the synthesis of SAL esters were described by Antoszczak *et al.* in 2014, based on the reaction between SAL and the appropriate alcohol in the presence of DCC, PPy (4-pyrrolidinopyridine) and *p*-TSA (*p*-toluenesulfonic acid) (Method A, 40-70% yield; Scheme 7), or based on direct alkylation of the carboxylate ion with the appropriate alkyl halide (chlorides or bromides) in the presence of 1,8-diazabicyclo[5.4.0]undec-7-ene (DBU) (Method B, Scheme 7). With method B, the yield increased up to 85%. The esterification methods show also a remarkable solvent dependence: dichloromethane was the best of all solvents tested for Method A and toluene for Method B.<sup>54</sup>

Often, the reversible masking of the carboxylic acid of SAL through esterification was adopted to enable selective derivatization of the C<sub>9</sub>, C<sub>20</sub>, and C<sub>28</sub> hydroxyl groups. In fact, it was demonstrated that the introduction of such protective groups enhances the stability of intermediates and facilitates both purification and characterization of intermediates in the selective *O*-acylation of SAL (Scheme 8).<sup>55</sup> In particular, a suitable protective group for the carboxylate, TMSEt (2-trimethylsilylethyl-), could be introduced in 61% yield, also on a multi-gram scale, using TMSEtOH and TCFH (*N'*-tetramethyl chloroformamidinium hexafluorophosphate) as the coupling reagent,<sup>56</sup> and then opportunely deprotected

with TBAF in THF. For an alternative to TBAF deprotection, allyl esters of SAL can also be prepared in 79% yield, using allyl bromide, in the presence of  $\text{Cs}_2\text{CO}_3$ , and the cleavage of this ester can be accomplished in moderate yield with  $\text{Pd}_2(\text{dba})_3$  (Scheme 8).



**Scheme 7.** Synthesis of SAL esters.



**Scheme 8.** Masking of the carboxylic acid of SAL through esterification.

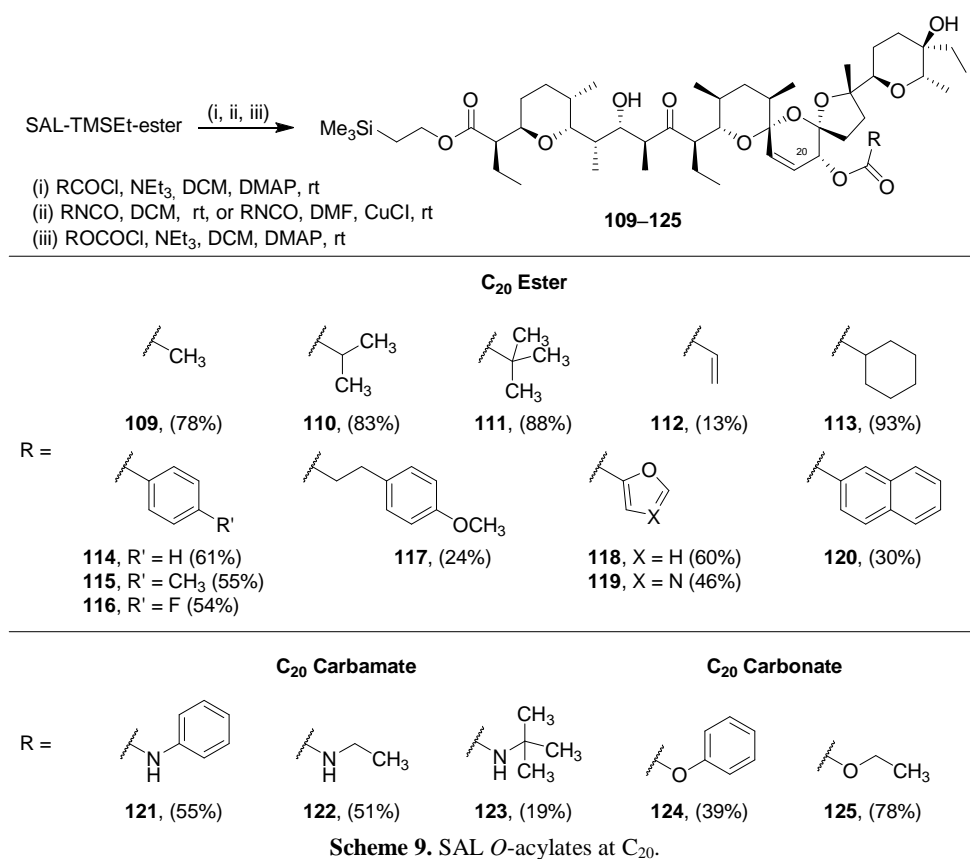
### 3.2. Modification of the hydroxyl groups

#### 3.2.1. Conjugates (*O*-acylates at C<sub>9</sub>, C<sub>20</sub>, and C<sub>28</sub>)

Selective synthetic strategies for the individual modification of the hydroxyl groups of SAL at C<sub>9</sub>, C<sub>20</sub>, and C<sub>28</sub> were recently reported.<sup>55</sup>

Pioneering work detailed the use of aliphatic acyl anhydrides to esterify the C<sub>20</sub> hydroxyl group,<sup>53,57</sup> but this method has limited applicability to unhindered aliphatic anhydrides (formyl, acetyl, propionyl, *n*-butyryl, *n*-valeryl) and low yield (Scheme 9).

In contrast to SAL or its sodium salt, protected SAL-TMSEt-ester can be reacted cleanly and selectively at the C<sub>20</sub> hydroxyl with a variety of acid chlorides (RCOCl), isocyanates (RNCO), and chloroformates (ROCOCl) to obtain C<sub>20</sub>-esters, carbamates, and carbonates (Scheme 9), respectively, while reactions of unprotected SAL (or its Na salt) with BzCl, DMAP, Bz<sub>2</sub>O gave either no reaction or extensive side product formation. The SAL-TMSEt-ester could be cleanly cleaved with TBAF, leading to SAL-derivatives selectively acylated at the 20-position.

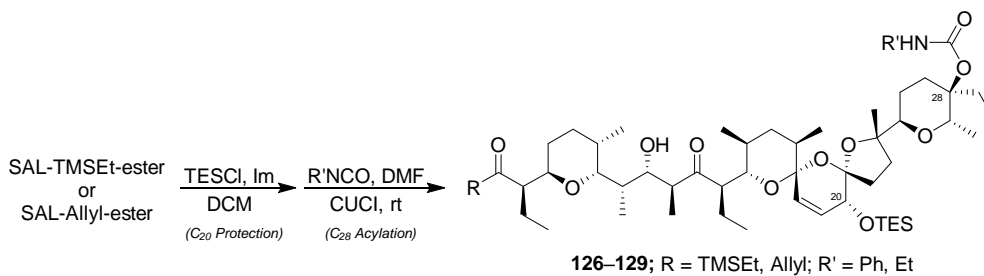


**Scheme 9.** SAL *O*-acylates at C<sub>20</sub>.

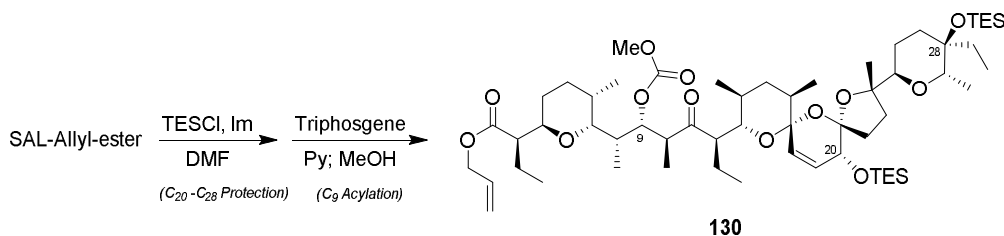
To enable selective derivatization of the C<sub>28</sub> alcohol, silyl groups were introduced on the C<sub>20</sub> hydroxyl

of SAL with TESC (triethylsilyl chloride) and imidazole in DCM, after opportunely protecting the carboxylic acid, while bis-silylation of both the C<sub>20</sub> and C<sub>28</sub> alcohols with TESC in DMF was necessary to modifying the least reactive C<sub>9</sub> hydroxyl.

Treatment of SAL, protected at C<sub>1</sub> (TMSEt or Allyl) and at C<sub>20</sub> (TES), with isocyanates (PhNCO and EtNCO), in the presence of CuCl and DMF, selectively carbamoylated C<sub>28</sub>-position. Removal of the protective groups with TBAF gave C<sub>28</sub>-carbamates (Scheme 10). Acylation of the C<sub>9</sub> alcohol was accomplished by reacting SAL, protected at C<sub>1</sub> (Allyl), at C<sub>20</sub> (TES) and C<sub>28</sub> (TES), with triphosgene followed by addition of methanol to give the corresponding methyl carbonates. Removal of the TES-protective groups with TBAF, followed by deprotection of the carboxylic group under Pd(0) catalyst gave the desired C<sub>9</sub>-carbonate (Scheme 11).



**Scheme 10.** SAL *O*-acylates at C<sub>28</sub>.



**Scheme 11.** SAL *O*-acylates at C<sub>9</sub>.

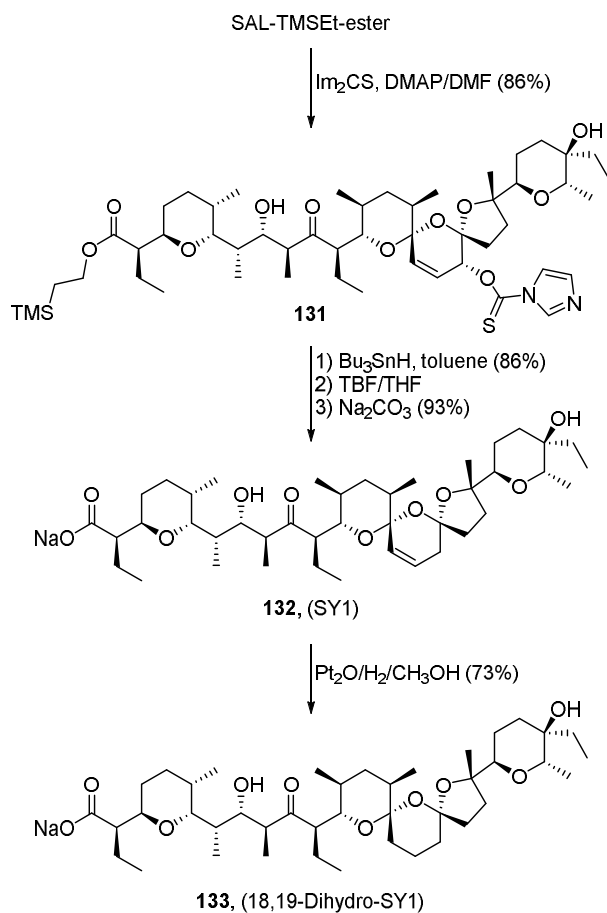
### 3.3. Reduction and oxidation

In an attempt to investigate the SAR of SAL and to evaluate the critical role of the carboxylic acid and the  $\beta$ -hydroxy ketone groups in forming cation-complex,<sup>53</sup> LiAlH<sub>4</sub> was used for the simultaneous reduction of the carboxylic acid and the  $\beta$ -hydroxy ketone groups, leading to 11-hydroxy-salinomycinol with a complete loss of activity. In addition, the selective reduction of the ketone group with NaBH<sub>4</sub> led to the 11-hydroxysalinomycin completely devoid of the antimicrobial and ion-transport activities.

The 18,19-dihydro-SAL showed a moderate decrease of their cation affinity. Whereas, the C<sub>20</sub>-keto-SAL, an  $\alpha,\beta$ -unsaturated ketone, obtained by the selective oxidation of the hydroxyl group at C<sub>20</sub> with active manganese dioxide, retained one-half of antibacterial activity compared with SAL.

### 3.3.1. 20-Deoxy SAL (SY1) and 18,19-dihydro SY1

SY1 is a natural product structurally related to SAL but deprived of the key C<sub>20</sub> hydroxyl group. SY1 is an intermediate in the biosynthesis of SAL,<sup>58</sup> and was isolated and characterized in 1977 as a minor constituent of the fermentation broth of *Streptomyces albus*.<sup>59</sup> Unlike SAL, SY1 is not readily available and its semi-synthesis starting from SAL-TMSEt-ester has been recently reported by Huang *et al.* (Scheme 12).<sup>60</sup>



**Scheme 12.** Semi-synthesis of SY1 and 18,19-dihydro SY1.

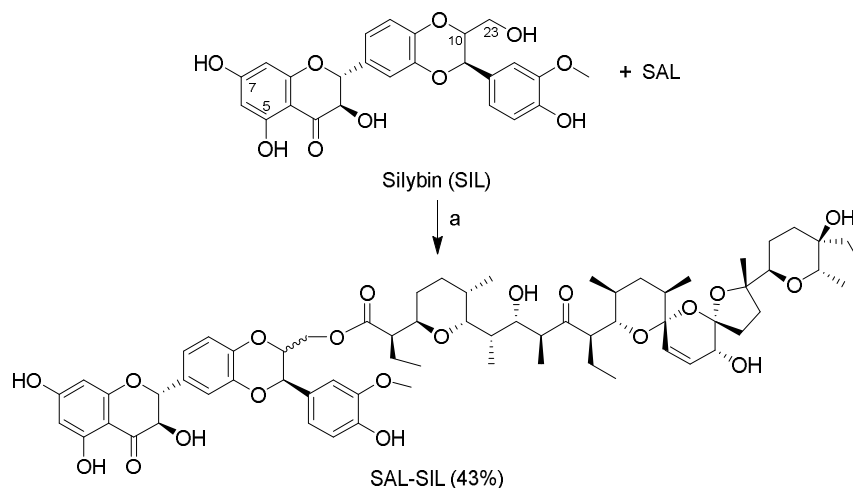
Treatment of SAL-TMSEt-ester with 1,1'-thiocarbonyldiimidazole (Im<sub>2</sub>CS) in DMF using stoichiometric DMAP gave the corresponding thiocarbamate in 86% yield with a complete selectivity for the allylic C<sub>20</sub> hydroxyl (Scheme 12). Allylic deoxygenation of thiocarbamate was achieved in 86% yield by a slow addition of Bu<sub>3</sub>SnH (excess) in toluene. The 18,19-unsaturated product **132** was obtained as a single regioisomer. The synthesis of SY1 (**132**) was completed by a fluoride-mediated cleavage of the TMSEt ester of **131** using TBAF in THF at ambient temperature. Following chromatographic purification and a Na<sub>2</sub>CO<sub>3</sub> wash (sat. aq), SY1Na was isolated in 93% yield as a single isomer, identical to the natural product by

optical rotation and IR. The synthesis of 18,19-dihydro SY1 (**133**) was achieved (74% yield) by hydrogenation of SY1Na over Adams catalyst (Scheme 12). The attempted hydrogenation of SAL-TMSEt-ester under the same conditions reduced the C<sub>18</sub>=C<sub>19</sub> unsaturation giving a complex mixture of products.

### 3.4. Salinomycin hybrid compounds

One of the current concepts in the anticancer drug design and development is the synthesis of new hybrid compounds (molecular hybridization/bioconjugation) of improved affinity and efficacy relative to those of the parent drugs. In order to produce hybrids molecules with superior efficacy compared with the single target drugs, to minimize the unwanted side-effects and allow a synergic action, the covalent combination of SAL with floxuridine,<sup>16</sup> Cinchona alkaloids<sup>18</sup> and silybin<sup>19</sup> (SIL) has been investigated.

The SAL-SIL bioconjugate was obtained by selective esterification of C<sub>23</sub>-OH primary alcoholic group of SIL with the carboxylic group of SAL (Scheme 13).



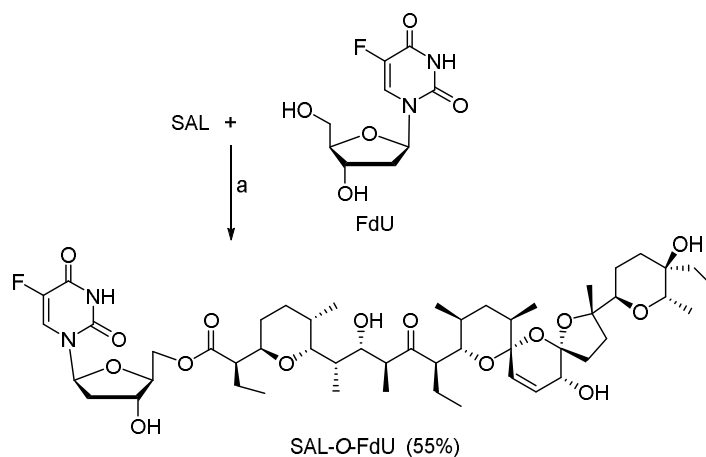
Reagents and conditions: SAL (1 eq), SIL (2.5 eq), DCC (1.5 eq), PPy (0.5 eq), *p*-TSA (0.23 eq), THF, 0 °C to rt, 24 h.

**Scheme 13.** Synthesis of SAL-SIL bioconjugate.

The esterification reaction of SIL with acyl chloride involved the most reactive C<sub>7</sub>-OH. Instead, the selective esterification at C<sub>23</sub>-OH was achieved by using acyl chloride in the presence of a Lewis acid.<sup>61</sup> The latter method cannot be employed for the conjugation of SIL with polyether ionophores because the several hydroxyl groups in SAL structure are very sensitive to acidic conditions as well as heating. The reaction between SAL and the primary C<sub>23</sub>-OH of SIL was performed under mild conditions using DCC, PPy, and *p*-TSA (Scheme 13). This procedure gave SAL-SIL bioconjugate in 43% yield as a mixture of two diastereomers (natural SIL is a mixture of two C<sub>10</sub> diastereoisomers, named Silybin A and Silybin B).

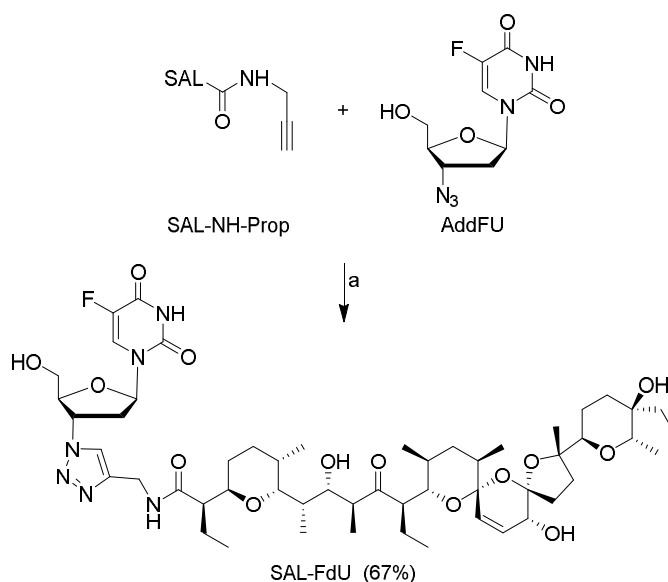
The first data on chemistry and the biological properties of SAL and modified nucleosides were reported by Huczyński *et al.*<sup>62</sup> Two different strategies have been explored from authors: the conjugation by

ester linkage starting from SAL and floxuridine (FdU) under mild condition (Scheme 14) and the conjugation by copper(I) catalyzed click Huisgen cycloaddition reaction performed between 3'-azido-2',3'-dideoxy-5-fluorouridine (AddFU) and SAL-propargyl amide (Scheme 15).



Reagents and conditions: a) DCC, PPy, *p*-TSA, DCM, 0 °C for 6 h, rt for 18 h.

**Scheme 14.** Synthesis of SAL-*O*-FdU.

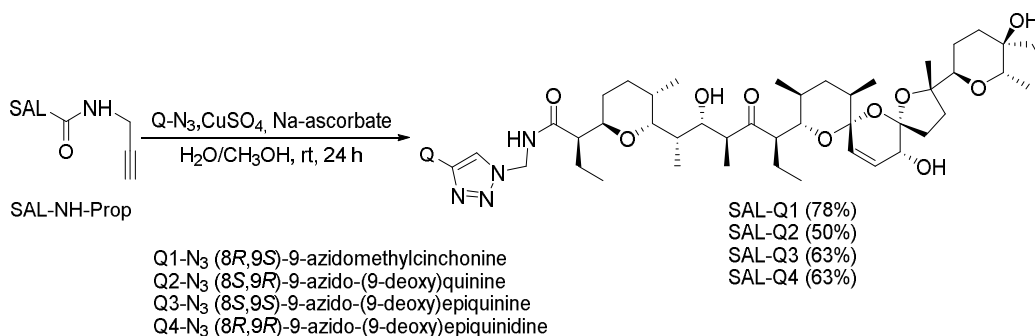


Reagents and conditions: CuSO<sub>4</sub>, sodium ascorbate, dioxane/water (3:1), rt, 12 h.

**Scheme 15.** Synthesis of SAL-FdU.

Although *Cinchona* alkaloids have no valuable anticancer activity (quinine IC<sub>50</sub>=40 μM and quinidine

IC<sub>50</sub>=113 μM in MCF-7 line), they have been used in reversing of multidrug resistance (MDR) in cancer patients treated with anticancer drugs such as doxorubicin, ethylprednisolone or vinblastine. On the basis of this consideration, the conjugation between SAL-propargyl amide with four *Cinchona* alkaloid azides has been investigated by Skiera *et al.* (Scheme 16).<sup>63</sup>



**Scheme 16.** Synthesis of SAL *Cinchona* alkaloid conjugates.

### 3.5. Metal complexes of salinomycin

SAL represents potential ligand able to bind metal cations due to the presence of oxygen atoms of various types (carboxylic, ether, hydroxyl) in the antibiotic molecule. The interaction of metal(II) ions with SALNa results in the formation of mononuclear complexes of a general composition of [M(Sal)<sub>2</sub>•(H<sub>2</sub>O)<sub>2</sub>]•nH<sub>2</sub>O (n=0 or 2) where the divalent cations replace Na<sup>+</sup> ions from the cavity of initial compound.<sup>64</sup> X-ray single crystal diffraction data for the mononuclear complexes of SAL with ions of Co(II), Ni(II), Cu(II) and Zn(II) were not provided.

On the basis of spectral data, the authors suggest that SAL mono-anions react with metal(II) ions in the equatorial plane of the complexes via terminal deprotonated carboxylic group and one of the secondary hydroxyl groups, both situated at the opposite ends of the ligand molecule. Two water molecules occupy the axial positions in the octahedron and their participation in various intramolecular hydrogen bonds supports the pseudo-cyclization of SAL similarly to the metal(II) di-monensinates which structures were refined in the solid state. SAL complexes of Cd(II) and Pb(II) were investigated by Ivanova *et al.*<sup>8</sup>

Cadmium(II) ion reacts with two carboxylate anions of SAL, extracting sodium ions from the cavity of the starting compound. Cadmium(II) di-SALate is expected to possess a distorted octahedral geometry similarly to the structures reported for the complexes of SAL with ions of Co(II), Ni(II), Cu(II) and Zn(II). In contrast, Pb(II) ions react with sodium SAL, extracting sodium ions from the ligand cavity, but forming a complex with a composition [Pb(Sal)(NO<sub>3</sub>)]. The extremely low solubility of this compound in water suggests that the nitrate ion is most probably coordinated in the inner coordination sphere of the metal center.

### 4. Ionophore properties

The biological activity of SAL as antibiotic is due to its ability to form complexes with metal cations and transport them across natural and artificial lipid bilayers. SAL is able to form complexes with both

mono- ( $K^+ > Na^+ > Cs^+$ ) and divalent ( $Str^{2+} > Ca^{2+}, Mg^{2+}$ ) cations.<sup>13</sup>

According to the X-ray studies, the complexed cation resides in a cage formed by oxygen atoms of the SAL with the hydrophobic skeleton wrapped around this cage; this arrangement, known as “tennis ball seam”, render the whole complex lipophilic. The complexation of metal cation is always accompanied by the formation of a pseudocyclic structure stabilized by “head-to-tail” intramolecular hydrogen bonds between the carboxylic group on one side of the molecule and hydroxyl groups on the other. The formation of the pseudocyclic structure facilitates transport of the cation across a lipid bilayer.<sup>65</sup>

SAL captures the cation on one side of the lipid bilayer in a stepwise process, replacing the solvate molecules one by one with its polar groups. The complex then moves across the membrane and releases the cation on the other side (Figure 4). The ionophore then diffuses back to the opposite side of the membrane, where the whole process can be repeated.<sup>65</sup>

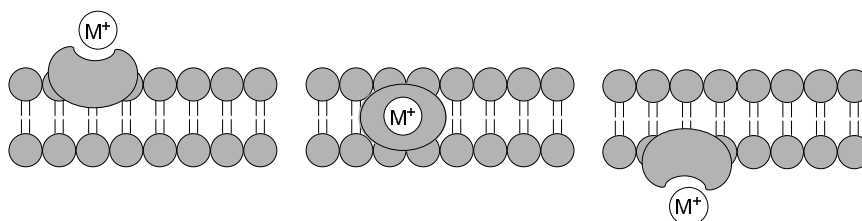


**Figure 4.** Transport of cations across lipid bilayer by ionophores.

The mechanism of cation transport by an ionophore is strongly dependent on the environment in which it occurs. In a neutral or slightly alkaline environment, the carboxyl group of ionophores is deprotonated ( $I-COO^-$ ) and the cation is transported by the electroneutral process (Figure 5a).

In this type of cation ( $M^+$ ) transportation, the polyether ionophore anion ( $I-COO^-$ ) binds the metal cation or proton ( $H^+$ ) to give a neutral salt ( $I-COO^-M^+$ ) or a neutral ionophore in the acidic form ( $I-COOH$ ), and only one uncharged molecule containing either a metal cation or proton can move through the cell membrane.<sup>66</sup> In 2012, Huczyński *et al.* showed that the process of complexation occurs in a non-alkaline environment (Figure 5b). The complex is formed with the polyether ionophore in its acidic form ( $I-COOH^+M^+$ ) instead of the polyether ionophore anion ( $I-COO^-M^+$ ) and the transport of cations is an electrogenic process.<sup>66</sup> The third type, termed biomimetic (Figure 5c) is realized by derivatives of polyether ionophores with block carboxylic function such as amides or esters.

An accurate study on the biologically active conformation of SAL-Na complex in membrane environments has been recently performed by Matsumori.<sup>67</sup> To mimic the membrane environment, and at the same time measuring the NMR spectra of SAL, phospholipidic isotropic bicelles composed by perdeuterated dimyristoylphosphatidylcholine (DMPC) and dihexanoylphosphatidylcholine (DHPC) were used at a ratio of 1:2.

The topological orientation of SAL within bicelles was determined both by a series of complexes 2D NMR studies and by monitoring the radical-induced relaxation of proton signals in the presence of doxyl-phospholipids. In particular, the conformation of SAL associated with isotropic bicelles was determined based on the NOEs and  $^3J_{HH}$  values obtained from the NOESY and DQF-COSY experiments, respectively.

These data were further used to set inter-proton distance and dihedral restraints in molecular modeling calculation studies.

From these studies emerged that the SAL structure in bicelles has a major alteration in the C<sub>24</sub>-C<sub>25</sub> bond; i.e., the orientation of the E-ring is significantly different from that in the crystal state or in organic solvents. In the bicelle structure, the dihedral angle of C<sub>23</sub>-C<sub>24</sub>-C<sub>25</sub>-O<sub>25</sub> takes a *gauche* conformation, while an *anti*-conformation is dominant in the crystal and solution structures. Moreover, the entire molecule of SAL is localized predominantly above the C<sub>5</sub> position of phospholipid acyl chains, i.e. the SAL is predominantly distributed in the DMPC-rich flat domain of the bicelle structure, with the carboxylate group that resides at the water-lipid interface.

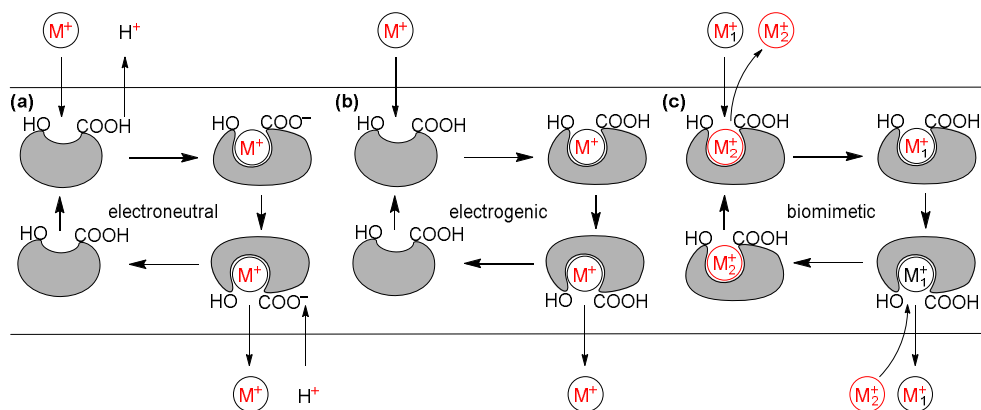


**Figure 5.** Electroneutral (a), electrogenic (b), and biomimetic (c) transport of cations by polyether ionophores.

In particular, the terminal E-ring is most likely to reside in a water accessible region and, from calculations, the solution structures (i.e. more stable conformers) have hydrophobic molecular surfaces because most of the oxygenated functional groups are directed inside to coordinate with the sodium ion; therefore, the structures are unstable in polar surroundings. In contrast, the bicelle structure has free oxygenated functionalities at the E-ring such as OH<sub>28</sub> and O<sub>25</sub> that can form hydrogen bonds with water and polar heads of phospholipids. Therefore, it seems reasonable to consider that the orientational change in the E-ring enhances molecular hydrophilicity, and consequently adjusts the molecule to more polar regions in the membrane. As a result of the orientational change in the E-ring, SAL cannot form an intramolecular hydrogen bond between OH<sub>28</sub> and O<sub>1</sub>, which plays a key role in forming closed conformations as reported in the crystal state and in organic solvents. In addition, the change in the E-ring prevents its ether oxygen from coordinating with the sodium ion. The resultant weak complexation of SAL with the sodium ion would promote the association/dissociation process of the ion; in contrast, there is little room for the exchange of the cation in the crystal state or in CDCl<sub>3</sub> because of the tight complexation.

The positional disorder of the sodium ion resulted from calculations also indicates the weaker complexation of the ion with SAL and the resultant shallow potential energy curve with respect to the position of the sodium ion. Combined with the result that SAL is predominantly located at the water-lipid

interface, it can be reasonably assumed that the positional disorder of the sodium ion represents the dynamic process of capture and release of the ion at the membrane surface. In other words, the conformation of SAL observed in bicelles would reproduce the structure around the membrane surface where metal ions are exchanging.

Because the previously reported crystal and solution structures seem to mimic those in hydrophobic environments, the use of the bicelle system allowed, for the first time, to observe the drug's structure that is in the process of association/dissociation of the ion at the water-lipid interface.

On the basis of these findings it is plausible to suppose that at the membrane surface, both termini of the SAL are closer to the water interface and the olefin portion facing the bicelle interior. While diffusing across the nonpolar membrane interior, the SAL molecule takes a closed conformation, by rotating the C<sub>24</sub>-C<sub>25</sub> bond.

Upon progression from the open state at the bicelle surface, where the sodium ion is weakly bound, to a closed conformation, where the sodium ion is more strongly bound, the sodium ion seems to move from one ligand sphere in the more open conformer environment to an altered ligand sphere in the closed conformer along a shallow potential well. Once closed, the molecular surface is hydrophobic and the metal ion is completely segregated from nonpolar lipid acyl.

## 5. Mechanism of action

Among similar ionophores, SAL showed the most effective activity not only *in vitro* model but likewise *in vivo* animal experiments with opportune xenograft tumor models in NOD/SCID and Balb/c mice.<sup>15</sup> Starting from this first work on the antitumoral activity, several *in vitro* (Table 2) and *in vivo* (Table 3) studies related to antiproliferative and apoptotic effects in cancer cells has been reported. Specifically, SAL induces apoptosis in CD4<sup>+</sup> T-cell leukemia cells collected from blood of patients with acute T-cell leukemia whereas failed to induce apoptosis in normal CD4<sup>+</sup> T-cells isolated from healthy humans, providing evidence that SAL selectively kills malignant cells.<sup>68</sup>

Furthermore, it has been reported an inhibitory effect of SAL on cell survival, colony growth, migration, and invasion of human non-small cell lung cancer A549 and LNM35 involving a marked increase in the expression of the pro-apoptotic protein NAG-1.<sup>69</sup>

In addition, SAL considerably sensitizes chemoresistant cancer cells or treated cells with irradiation providing an increased responsivity and synergistic antitumor activity to drugs and irradiation treatments.<sup>70-77</sup> Despite several *in vitro* and *in vivo* studies on cancer cell proliferation to date reported, the exact mechanism of anticancer activity of SAL remains to be explained. Several biomolecular pathways have been reported to provide evidence of SAL antiproliferative and apoptotic cell-killing activity in different cancer cell lines, involving Wnt/ $\beta$ -catenin signalling<sup>78</sup> and induction of a marked increase in the expression of the pro-apoptotic protein NAG-1 in chronic lymphocytic leukemia cells or in human non-small cell lung cancer A549 and LNM35.<sup>69,79</sup>

Moreover, inhibition of oxidative phosphorylation<sup>14</sup> or interference in ABC Transporters P-glycoprotein/MDR1 in glioma cancer or human leukemia stem cells has been demonstrated.<sup>80</sup> Recent studies showed a strong mTORC1 signaling antagonist in breast and prostate cancer cells and as an initiator of autophagy in tumor cells.<sup>78,81,82</sup>

Conversely, Klose *et al.* described that SAL is also able to suppress late stages of autophagy, leading to accumulation of dysfunctional mitochondria with increased production of reactive oxygen species (ROS).<sup>83</sup>

**Table 2.** *In vitro* antitumoral activity of SAL.

Cell Line	Cancer Type	Pharmacological activity	Ref.
A-549 LNM35	Lung cancer	The IC <sub>50</sub> concentrations at 24 h are in the range of 5 to 10 $\mu$ M of SAL for both cell lines. After 48 h treatment, the IC <sub>50</sub> concentrations decreased to the range of 1.5 to 2.5 $\mu$ M of SAL with 90% inhibition of cell viability in both cells at the concentration of 50 $\mu$ M.	69
MCF-7 MDA-MB-231 T47D	Breast cancer	The IC <sub>50</sub> at 24 h is approximately 40 $\mu$ M for the MCF-7 and T47D, while the same concentration gives only about 35% inhibition of proliferation in the MDA-MB-231 cells. Following 48 h treatment, IC <sub>50</sub> is 15 $\mu$ M for the MCF-7 and T47D, and about 35 $\mu$ M for the MDA-MB-231 cells. On the other hand, T47D is the most sensitive cell line among the breast cancer cell lines tested.	82,84
HEK293	Chronic lymphocytic leukemia	Incubation of the malignant lymphocytes with SAL induces apoptosis within 48 h, with a mean IC <sub>50</sub> of 230 nM. Under the same conditions, SAL fails to induce apoptosis in peripheral blood mononuclear cells at 100-fold higher concentrations.	79
EGI-1 Mz-ChA-1 TFK-1	Cholangiocarcinoma	After 24 h treatment of Mz-ChA-1, TFK-1 and EGI-1 cancer cells with 5 $\mu$ M of SAL, about 65%, 86% and only 10% of these cells undergo apoptosis process, respectively. After increasing the dose of SAL to 10 $\mu$ M, significant changes are not observed in Mz-ChA-1 and TFK-1 cells, but number of EGI-1 cells that compliant an apoptosis process increases to about 18%.	85
RKO SW480 SW620	Colorectal cancer	At the 10 $\mu$ M concentration of SAL, the cell viability decreases by 95% in comparison to the solvent control in all colorectal cancer cell lines. The decrease in viability is highly significant, post-hoc testing reveals that the difference between solvent control and SAL treatment is significant for all concentrations >1 $\mu$ M after 72 h.	82
T98G U251 U87MG	Glioblastoma	Dose-response experiments carried out on cells exposed to increasing concentrations of SAL (from 0.6 to 10.0 $\mu$ M) show a decrease of viable cells, marked in U87MG cells as well as moderate in T98G and U251 cells. Maximal effects	74

		are observed at a SAL concentration corresponding to 5-10 $\mu\text{M}$ . On the other hand, the addition of TRAIL, even at low concentrations, i.e. at 10 ng/mL, to 1.2 $\mu\text{M}$ of SAL causes a marked reduction of viable cells.	
BEL-7402 HepG2 Huh7 LM3 SMMC-7721	Hepatocellular cancer	The $\text{IC}_{50}$ value is about 14.7 $\mu\text{M}$ , 18.6 $\mu\text{M}$ and 17.1 $\mu\text{M}$ for HepG2, SMMC-7721 as well as BEL-7402 cell lines after 24 h treatment of SAL, respectively. These values decrease to about 10.2 $\mu\text{M}$ , 15.3 $\mu\text{M}$ , and 13.8 $\mu\text{M}$ after 48 h treatment of SAL for these cells. On the other hand, treatment of hepatocellular cells in the combination of SAL with 5-fluorouracil for 48 h results in a decrease in cell viability, which is greater than either SAL and 5-fluorouracil alone.	75,83, 86,87
CNE-1 CNE-2 CNE-2/DDP	Nasopharyngeal cancer	SAL at a concentration of 8 $\mu\text{M}$ inhibits about 53.0%, 48.0% and 42.3% of the survival of CNE-1, CNE-2 and CNE-2/DDP cells after 48 h treatment, respectively. When CNE-1 cells are exposed for 72 h to 16 $\mu\text{M}$ of SAL, the inhibition ratio is up to 70%.	88
HEK-293T MG-63 U2OS	Osteoblastoma	No significant cell viability loss is observed with treatment of SAL at a concentration lower than 1 $\mu\text{M}$ . On the other hand, 48 h treatment with 10 $\mu\text{M}$ of SAL reduces the viability of U2OS, MG-63 and HEK-293T cells to about 50%, 53%, and 52%, respectively.	89
OVCAR-8 OV2008	Ovarian cancer	The viability of OVCAR-8 cell line is reduced to about 53% and 45% after 72 h treatment of 4 $\mu\text{M}$ as well as 8 $\mu\text{M}$ of SAL, respectively. On the other hand, $\text{IC}_{50}$ (95% confidence interval) of SAL on OV2008 cell line for 24, 48 and 72 h treatment is 7.44, 4.78 as well as 3.20 $\mu\text{M}$ , respectively.	90,91
A2780	Ovarian epithelial cancer	SAL induces a moderate pro-apoptotic effect on A2780 cells, particularly evident at days 2-3 of culture and at SAL dosages of 1-5 $\mu\text{M}$	92
DU-145 LNCaP PC-3 VCaP	Prostate cancer	At 1.33 $\mu\text{M}$ concentration of SAL LNCaP cells manifest a stronger inhibition – viability reduced to about 55%, 38%, 35% and 22% (after 12, 24, 36 and 48 h, respectively), whereas >50% of PC-3 and DU-145 cells remain viable after 36 h treatment of SAL and even at 48 h >30% of PC-3 cells as well as >50% of DU-145 cells remain viable. On the other hand, SAL is the most effective in inhibiting VCaP cells ( $\text{EC}_{50}$ =380 nM), whereas non-malignant prostate epithelial RWPE-1, EP156T as well as PrEC cells are nonresponsive ( $\text{EC}_{50}$ >10 $\mu\text{M}$ ).	93,94

Apoptosis induced by anticancer drugs is related to induction of p53 protein expression. Nevertheless, in several human cancer cells, apoptotic cell death induced by SAL was not related to the expression of this protein, proteasomes or caspase activity but to a separate apoptotic pathway with no change in cell cycle.<sup>68</sup>

**Table 3.** *In vivo* antitumoral activity of SAL.

Mice/Humans	Cancer Type	Pharmacological activity	Ref.
Mice	Breast cancer	Animals were administered either ethanol (vehicle), SAL (5 mg/kg) or Paclitaxel (5 mg/kg) daily by intraperitoneal injection for 5 weeks. While palpable tumors developed in vehicle-treated mice within about 1.5 weeks, Paclitaxel and SAL treatment both delayed palpable tumor formation by about 2 weeks. Subsequent tumor size in SAL-treated mice was reduced relative to tumors in vehicle-treated mice. Four weeks after cancer cell injection, tumors were analyzed for the presence of surviving CSCs with <i>in vitro</i> tumor sphere formation assays. Tumors from the Paclitaxel-treated cohort had a 2-fold increase in tumor sphere forming cells relative to either SAL- or vehicle-treated cohorts. Tumors from SAL-treated mice had increased necrosis and apoptosis compared to comparably sized tumors from vehicle-treated mice. Viable cancer cells in tumors from SAL-treated mice were mostly restricted to the periphery of the tumor mass.	15
Mice	Endometrial cancer	Animal experiments were performed on 5-week-old nude mice and the tests were conducted for 6 months. The size of the tumor was measured every week and the weight of each mouse tested was recorded once a week. After palpable tumors (1 cm <sup>3</sup> ) had developed, 0.26 μM of SAL or DMSO was injected into the tumors. Tumors in DMSO-treated mice continued to grow, but tumors in SAL-treated mice stopped growing. Tumor size in SAL-treated mice was reduced compared with tumors in DMSO-treated mice.	96
Mice	Hepatocellular cancer	Animal experiments were performed on 6-week-old male nude mice. Saline, 5-fluorouracil (8 mg/kg), SAL (4 mg/kg) as well as combination of 5-fluorouracil (8 mg/kg) and SAL (4 mg/kg) were used in these tests. Observations of the anti-tumor effects of the substances tested were carried out for 4 weeks. The subcutaneous tumor volume was reduced in the combination therapy group compared to other three groups. The anti-tumor effect was observed by measuring tumor diameter in the animals tested twice per week. The relative tumor proliferation rate was slower and the tumor-growth inhibition rate was greater in the	75

		combination therapy than in the other three groups.	
Mice	Nasopharyngeal cancer	Animal experiments were performed on 4-week-old male nude mice. After tumors grew to about 4 mm, mice were randomly divided into a control group and a SAL group (10 mg/kg). Drugs were given by intraperitoneal injection daily for 2 weeks. The animal weight and tumor volumes were monitored every other day. Assessment of tumor volume showed that the SAL-treated group showed delayed tumor growth compared to the control group. The tumors were smaller in the experimental group than in the control group.	88
Mice	Osteosarcoma	Animal experiments were performed on 6-8-week-old mice. Tests were conducted for 33 days and tumor volumes were monitored at day 15 and then every 2 days. The mice were treated with 5 mg/kg of SAL or normal saline solution intraperitoneally every day. SAL reduced tumor growth and acted synergistically with chemo-drug Adriamycin. SAL treatment had a minimal effect on the body weight of nude mice in comparison with treatment using normal saline solution.	17
Mice	Ovarian cancer	Animal experiments were performed on 6-week-old female mice. The two experimental groups were administered SAL (5 mg/kg) and 5% ethanol (vehicle), respectively, by intraperitoneal injection every other day for three weeks. The size of the tumor was measured every two days. Compared with the vehicle-treated controls, a significant reduction in the tumor volume was observed in the SAL-treated mice. At the end of the test, the tumor volume of SAL-treated and the control groups, in the C13 tumor model, was $84.2 \pm 30.8$ as well as $252.5 \pm 63.4$ mm <sup>3</sup> , respectively.	97
Humans	Invasive breast, head, neck and ovary carcinoma	Patients were administered 200–250 µg/kg of SAL intravenously every second day for three weeks. Two cases are described in literature in detail. The first was a 40-year-old female patient with metastatic (bone and subcutaneous) invasive ductal breast cancer and the second was an 82-year-old female patient with advanced and metastatic (pelvic lymphatic metastasis) squamous cell carcinoma of the vulva. In both cases, the administration of SAL resulted in inhibition of cancer disease progress over an extended period of time. Acute side effects were rare and the serious long-term adverse side effects were not observed.	16

Recently, it has been reported that in breast cancer stem-like cells an apoptosis-independent pathway induced the antitumor activity by downregulation of cyclin D1 and increasing p27<sup>kip1</sup> nuclear accumulation. Mammosphere formation assays revealed that SAL suppresses self-renewal of ALDH1-positive breast cancer stem cells and downregulates the transcription factors Nanog, Oct4, and Sox2. *In vivo* study on MDA-MB-231-derived xenografts with TUNEL analysis, revealed a significant reduction in tumor growth with a marked downregulation of ALDH1 and CD44 levels, but apparently without the induction of apoptosis.<sup>95</sup>

However, all these pharmacological, as well as biological effects, were related to up or down-regulation of peculiar gene expression related to typical cancer cell lines but not provide a clear specific biomolecular target interactions. The aptitude of this ionophore, to unsettle intracellular ion balance and to lower intracellular pH, induced inhibition of DNA synthesis.<sup>98</sup> Moreover, the strong affinity for potassium cations promotes the outflow of these ions reducing internal concentration from the mitochondria as well as cytoplasm. Additionally, in many human cancer cells an overexpression of potassium channels was reported showing a very important role in the cell cycle progression, proliferation, and apoptosis of tumor cells.<sup>99</sup>

Specifically, recent studies addressed to the direct effect of SAL compared to Valinomycin and Nigericin on mitochondria function of primary human healthy cells, cancer cells, and cancer stem cell-like.<sup>100</sup> The obtained results showed that SAL acts in intact cells as an K<sup>+</sup>/H<sup>+</sup> antiporter and directly influences mitochondrial function in a few minutes upon addition, suggesting the hypothesis that polyether ionophore antibiotics contribute to apoptosis induction by a common mechanism.

However, additional studies will be necessary to closely delineate the factors contributing to the moderate to high selectivity of SAL and Nigericin toward different cancer cells, given that these ionophores a priori affect mitochondrial functions independently of differences in signaling pathways.

## 6. Structure-activity relationships

Ionophore SAL and others polyether showed antibiotic activity principally towards Gram-positive bacteria such as *Staphylococcus aureus* and anti-mycobacterial, anti-fungal and anti-protozoal activity. The first data regarding biological activity of SAL derivatives are reported by Huczyński *et al.* in 2012.<sup>52</sup> The synthesis and antimicrobial properties of only an ester (**91**)<sup>52</sup> and eight amides (**49-64**)<sup>45</sup> have been reported (Schemes 6 and 7). Subsequently, the same authors provide the synthesis and antibacterial activity of a new series of SAL amides and esters.<sup>47,54</sup> The results showed that some esters and amides (**61**, **53-60**, and **94**) are active against standard strains of *S. aureus*, with a comparable or lower activity to that of unmodified SAL. However, trifluoroethyl ester (**99**) showed higher antibacterial activity than unmodified SAL and the antibacterial drug ciprofloxacin. Regarding these new esters and amides derivatives, no anti-mycobacterial, antifungal and antiprotozoal activity were reported to date.

The principal reasons why SAL received a big consideration is related to anticancer activity towards several chemo- and radio-resistant CSCs that often induce a recurrence of the disease. Several types of natural compounds have been used as antitumor agents, both in their original, chemically unmodified forms as well as in the synthetically transformed forms.<sup>66</sup> Therefore, a pursued path to discover new effective anticancer drugs is a chemical modification of naturally occurring substances with proven high biological activity, such as polyether SAL.

Recently, starting from the first data reported by Huczyński *et al.*, the antiproliferative properties of a series of amides (Scheme 6, **49-90**; Figure 3, **92-94**) and esters (Scheme 7, **95-106**) as well as *O*-acylated derivatives (Schemes 8 and 9, compounds **107-125**) of SAL have been reported.<sup>45,47,48,52,54,55</sup> Anticancer activity of SAL amides (**49-90**) and esters (**95-106**) were determined in vitro against human leukemia cells sensitive and resistant to vincristine (HL-60 and HL-60/vincristine, respectively), human colon cancer cells sensitive and resistant to doxorubicin (LoVo and LoVo/DX), and against normal murine embryonic fibroblasts (BALB/3T3). Substantially, all tested derivatives showed changed antiproliferative activity related to type of ester or amide moiety and the considered cell line. However, all SAL derivatives strongly or moderately inhibit the MDR of used cancer cell lines and the level of this effect depends on the chemical nature of SAL derivatives.<sup>48</sup> Specifically, 4-fluorophenethyl- (**63**), dopamine- (**64**), aniline- (**61**) and 2-(1*H*-indol-3-yl)ethan-amides showed the better antiproliferative activity of the series against LoVo/DX. Regarding ester derivatives, preliminary SAR studies displayed that the most potent anticancer compounds among SAL esters are those which contain trifluoroethyl ester group (**99**) or a short aliphatic chain (**96**),  $\alpha$ -naphthylmethyl (**104**), or polar di-*o*-nitrobenzyl (**103**) ester substituents.<sup>54</sup> The highest antiproliferative activity against all cell lines tested was related to trifluoroethyl ester (**99**) with an IC<sub>50</sub> lower with respect to unmodified SAL and potent anticancer drugs cisplatin and doxorubicin (Table 4). In addition, amides **60** and **63** and ester derivatives **91**, **96**, **99** and **104** are less toxic against normal embryonic murine fibroblasts BALB/3T3 cell line (IC<sub>50</sub>>20  $\mu$ M) than the commonly used anticancer drugs cisplatin and doxorubicin.

**Table 4.** Antiproliferative activity of SAL and its selected amides and esters against human leukemia cell line sensitive and resistant to vincristine (HL-60 and HL-60/vinc), human colon cancer cell line sensitive and resistant to doxorubicin (LoVo and LoVo/DX) and normal murine embryonic fibroblasts (BALB/3T3).<sup>47,48,54</sup>

Compound	IC <sub>50</sub> $\pm$ SD ( $\mu$ M)				
	HL-60	HL-60/vinca	LoVo	LoVo/DX	BALB/3T3
SAL	0.44 $\pm$ 0.16	3.44 $\pm$ 0.32	1.11 $\pm$ 0.15	6.23 $\pm$ 1.72	28.08 $\pm$ 4.63
<b>51</b>	3.88 $\pm$ 0.04	5.31 $\pm$ 0.68	4.04 $\pm$ 0.17	3.26 $\pm$ 0.61	8.21 $\pm$ 1.14
<b>58</b>	3.52 $\pm$ 0.13	4.31 $\pm$ 0.52	3.45 $\pm$ 0.26	2.78 $\pm$ 0.47	9.98 $\pm$ 4.71
<b>60</b>	3.08 $\pm$ 0.25	6.87 $\pm$ 0.27	6.24 $\pm$ 1.08	5.65 $\pm$ 1.12	25.47 $\pm$ 4.24
<b>61</b>	3.79 $\pm$ 0.07	4.31 $\pm$ 0.53	4.11 $\pm$ 0.15	3.21 $\pm$ 0.49	7.08 $\pm$ 1.40
<b>62</b>	3.63 $\pm$ 0.25	6.02 $\pm$ 0.72	4.02 $\pm$ 0.17	3.31 $\pm$ 0.76	7.26 $\pm$ 1.02
<b>63</b>	2.26 $\pm$ 0.24	6.74 $\pm$ 1.15	4.09 $\pm$ 0.14	2.34 $\pm$ 0.49	45.80 $\pm$ 20.94
<b>64</b>	2.77 $\pm$ 1.11	6.88 $\pm$ 1.08	3.88 $\pm$ 0.24	4.26 $\pm$ 0.74	5.69 $\pm$ 2.17
<b>91</b>	1.84 $\pm$ 0.37	5.25 $\pm$ 0.55	4.11 $\pm$ 0.20	6.61 $\pm$ 1.12	31.90 $\pm$ 5.33
<b>96</b>	3.58 $\pm$ 0.45	4.15 $\pm$ 1.50	4.04 $\pm$ 0.09	3.99 $\pm$ 0.06	24.32 $\pm$ 7.27
<b>99</b>	0.47 $\pm$ 0.22	3.05 $\pm$ 0.38	0.78 $\pm$ 0.24	0.80 $\pm$ 0.07	23.82 $\pm$ 6.49
<b>104</b>	3.73 $\pm$ 0.21	9.33 $\pm$ 1.47	7.34 $\pm$ 0.35	4.70 $\pm$ 0.28	35.80 $\pm$ 1.66
Doxorubicin	0.06 $\pm$ 0.02	0.91 $\pm$ 0.06	0.38 $\pm$ 0.07	12.14 $\pm$ 1.93	1.91 $\pm$ 0.74
Cisplatin	1.12 $\pm$ 0.13	5.98 $\pm$ 0.40	2.40 $\pm$ 0.37	4.18 $\pm$ 1.20	8.40 $\pm$ 1.40

Recently, Borgström *et al.* reported the synthesis and the evaluation of antiproliferative activity of the deprotected *O*-acylated derivatives (**109-125**) towards two human breast adenocarcinoma cell lines (JIMT-1 and MCF-7). The C<sub>20</sub>-acylated analogs display an activity higher than SAL sodium salt (IC<sub>50</sub>=0.52-0.59 μM and IC<sub>50</sub>=0.09-0.81 μM for SAL sodium salt and its C<sub>20</sub>-acylated analogs, respectively). Moreover, preliminary SAR studies on C<sub>20</sub>-acylated analogs displayed that a reduced steric hindrance on carboxylate, carbonate and carbamate substituents increases the antiproliferative activity on these cell lines [deprotected acetate **109** (IC<sub>50</sub>=0.11 μM), ethyl carbonate **125** (IC<sub>50</sub>=0.09-0.13 μM) and ethyl carbamate **122** (IC<sub>50</sub>=0.16-0.26 μM)]. The analogs deprived of stabilizing interaction between the carboxylate and the C<sub>9</sub>-hydroxyl group exhibit reduced activity (IC<sub>50</sub>=1.67-1.85 μM). The preserved anticancer activity of the C<sub>28</sub> carbamates (IC<sub>50</sub>=0.62-5.56 μM) suggests that in biological membranes, C<sub>28</sub>-hydroxyl group does not contribute to the ion binding of SAL sodium salt by hydrogen bonding to the carboxylate.<sup>55</sup>

### 7. Salinomycin as a drug for targeting human cancer stem cells

Cancer stem cells (CSCs) are a subpopulation of cancer cells that have been invoked in recurrence, multi-drug resistance, and metastasis of cancer.<sup>16</sup> CSCs are cells localized within solid tumours, or in hematological cancers, that have traits associated with normal stem cells, and have the potential to give rise to all cell types found in particular cancer.<sup>101</sup> Given their ability to evade chemo- and/or radiotherapy, these cells can survive and usually persist in tumours for a substantial length of time as a distinct population, and can eventually cause relapse and metastasis by generating new tumours.<sup>102</sup> Despite it is currently not known whether all cancer types contain subpopulations of CSCs and the earlier controversies about their role and existence, CSCs are now an appealing target in the fight against neoplastic diseases.

Following the discovery of SAL as a CSCs killer, the pharmacological effects of SAL have been tested in several models *in vitro* and *in vivo*.<sup>103</sup> SAL targeting CSCs in different types of cancers, including gastric cancer, lung adenocarcinoma, osteosarcoma, colorectal cancer, and squamous cell carcinoma.<sup>6</sup>

The mechanism by which SAL influences the CSC population is not fully understood.<sup>7,8</sup> Proposed modes of action include inhibition of P-glycoprotein gp170,<sup>92</sup> interference of the Wnt signaling cascade,<sup>79</sup> increased DNA damage and reduction of the protein p21 level,<sup>11</sup> overcoming ABC transporter-mediated multidrug and apoptosis resistance,<sup>104</sup> increasing oxidative stress,<sup>93</sup> and increasing levels of reactive oxygen species.<sup>82,94</sup>

One important caveat for the potential clinical use of SAL is its severe toxicity. Some incidents were documented in humans for accidental ingestion of SAL at relatively high doses. In these cases, as well as in cases of animal poisoning, a significant neuromuscular toxicity was observed. In line with these findings, a recent study provided evidence that SAL at the micromolar range (1-10 μM) causes *in vitro* a cytotoxic effect on murine dorsal root ganglia neurons by means of calpain and cytochrome c-mediated caspase 9 and subsequent caspase 3 activations. Therefore, in view of a possible clinical use of this antibiotic it is particularly important to identify drug combinations, allowing both to potentiate the antitumor activity of SAL and to decrease the concentration of this drug.<sup>74</sup>

Currently, the research in this field is focused on the development of biologically active bioconjugates of SAL such as amides, esters, carbamates and carbonates.<sup>51,62</sup> Moreover, different SAL bioconjugates with floxuridine,<sup>62</sup> Cinchona alkaloids<sup>63</sup> and silybin<sup>105</sup> have been reported.

The C-ring-modified derivatives of SAL (SY1 **132**, and 18,19-dihydro SY1 **133**) exhibit very similar activities against human breast JIMT-1 and HCC1937 cancer cell lines, but are less active than the parental ionophore. SAL sodium salt is found more efficient than these two analogs in reducing the proportion of CD44<sup>+</sup>/CD24<sup>-</sup> cells, but all compounds target this phenotype with substantially complete selectivity in JIMT-1 cell line at concentrations below the respective IC<sub>25</sub>. Similar biological profiles of SAL sodium salt and these two analogs suggest that they act through a common mechanism.<sup>60</sup>

This high anti-tumor activity of SAL derivatives may be connected with the Warburg effect and/or with different mechanisms of ion transport by polyether antibiotics. Three different ion transport mechanisms through the biological membranes realized by polyether antibiotics are described in literature: (a) electroneutral transport, when the transmembrane potential is maintained, (b) electrogenic transport, when the transmembrane potential is changed and (c) biomimetic transport implemented by polyether antibiotics with the chemically modified carboxyl group.<sup>106</sup>

The Warburg effect is observed in the most cancer cells, which predominantly produce energy by a high rate of glycolysis followed by lactic acid fermentation in the cytosol, rather than by a comparatively low rate of glycolysis followed by oxidation of pyruvate in mitochondria. It has been postulated that this change in metabolism is the fundamental cause of cancer diseases.<sup>107</sup>

The high anti-cancer activity of SAL derivatives is probably connected with the mechanism of cations transport realized by such compounds. In cancer cells that are highly acidic, the most common electroneutral transport cannot be effectively carried out, because the carboxyl group does not undergo deprotonation. Biomimetic transport is then preferred.

The antiproliferative activity of SAL-SIL bioconjugate was tested (Table 5) in various human cancer cells, including those that display multidrug resistance (MDR). SAL-SIL exerted antiproliferative activity at micromolar concentrations (IC<sub>50</sub> 14.01 μM) and a relatively low toxicity against normal murine embryonic fibroblast cell line (IC<sub>50</sub>>30 μM). It is worth noting that SAL-SIL was more active than cisplatin against LoVo (human colon adenocarcinoma) and LoVo/DX (doxorubicin-resistant subline) cancer cell lines and less active than doxorubicin against HepG2 (human liver cancer). None specific assay was reported about the antiproliferative effects of SAL-SIL on CSCs. The obtained data suggest that the proposed conjugation between SAL and SIL not induces the expected synergic effects. Moreover, it is not clear if the biological activity is due to SAL-SIL bioconjugate or two starting compounds originated *in vivo* by cellular carboxylesterases.

**Table 5.** IC<sub>50</sub> (μM) on LoVo, LoVo/DX, HepG2, and BALB/3T3 cancer cell lines.

Compound	Cancer cells			Normal cells
	LoVo	LoVo/DX	HepG2	BALB/3T3 <sup>a</sup>
SAL	0.61	0.52	12.44	35.18
SIL	72.32	76.97	73.78	121.08
SAL-SIL	3.63	3.93	14.01	30.10
Doxorubicin	0.28	6.73	0.77	0.53
Cisplatin	4.40	5.67	8.93	12.43

<sup>a</sup>Normal murine embryonic.

The results of biological studies on two examples of nucleoside and SAL bioconjugates (Sal-FdU and SAL-*O*-FdU) indicate that the antiproliferative effects strictly depend on chemical nature of the conjugates. SAL-*O*-FdU conjugate obtained by esterification reaction showed higher anticancer activity than the corresponding SAL-FdU obtained by the 'click' reaction. Moreover, SAL-*O*-FdU exhibits also better anticancer activity than its precursors. The SAL-*O*-FdU displayed antiproliferative activity in various cell types in the low micromolar range and showed selectivity index from 11.45 up to 87.24. Moreover, SAL-*O*-FdU broke the drug resistance of LoVo/DX cancer cells. The higher activity of SAL-*O*-FdU conjugate is probably connected with high cleavage of ester group by cellular carboxylesterases which lead to the presence of free floxuridine and SAL that kill the cancer cells acting with independent mechanisms.

The *in vitro* antiproliferative effect of *Cinchona* alkaloid conjugates (SAL-Q1, SAL-Q2, SAL-Q3, SAL-Q4), were evaluated for three cancer (LoVo, LoVo/DX, and HepG2) and one normal cell lines. The activities were compared with their precursors (SAL, Q1–Q4) and two reference anticancer drugs: doxorubicin and cisplatin. The synthesized conjugates exerted antiproliferative activity at micromolar concentrations (IC<sub>50</sub> from 2.05 to 19.57 µM) against the three human cancer cell lines and, simultaneously, relatively low toxicity against normal murine embryonic fibroblast cell line. None of the four conjugates exceeded the very high anticancer activity of parent SAL (IC<sub>50</sub> from 0.52 to 12.54 µM).

## 8. Conclusions

Natural products are the original source of well-known and commonly used drugs. SAL ionophore is a unique natural compound that exhibit a broad spectrum of biological activities, including antibacterial, antiviral, and anticancer ones. High biological activity of SAL is related to its chemical structure, as well as the ability to form complexes with mono- and divalent metal cations and transport them across lipid membranes. It results in a disturbance of the natural cation concentration gradient and intracellular pH change, leading to mitochondrial injury, cell swelling, vacuolization and, as a consequence, programmed cell death. Since the easiest method for preparing biologically effective compounds is the chemical modification of substances with proven high biological activity, a plethora of SAL derivatives were synthesized and biological assays clearly demonstrated that some of these derivatives showed an enhanced antimicrobial and anticancerous activity with respect to SAL.

## References

1. Dutton, C. J.; Banks, B. J.; Cooper, C. B. *Nat. Prod. Rep.* **1995**, *12*, 165.
2. Callaway, T. R.; Edrington, T. S.; Rychlik, J. L.; Genovese, K. J.; Poole, T. L.; Jung, Y. S.; Bischoff, K. M.; Anderson, R. C.; Nisbet, D. J. *Curr. Issues Intest. Microbiol.* **2003**, *4*, 43.
3. Gabrielli, C.; Hemery, P.; Letellier, P.; Masure, M.; Perrot, H.; Rahmi, M. I.; Turmine, M. *J. Electroanal. Chem.* **2004**, *570*, 291.
4. Rochefeuille, S.; Jimenez, C.; Tingry, S.; Seta, P.; Desfours, J. P. *Mater. Sci. Eng. C-Bio. S.* **2002**, *21*, 43.
5. Miyazaki, Y.; Shibuya, M.; Sugawara, H.; Kawaguchi, O.; Hirsoe, C. *J. Antibiot. (Tokyo)* **1974**, *27*, 814.
6. Kinashi, H.; Otake, N.; Yonehara, H.; Sato, S.; Saito, Y. *Tetrahedron Lett.* **1973**, 4955.
7. Davis, A. L.; Harris, J. A.; Russell, C. A. L.; Wilkins, J. P. G. *Analyst* **1999**, *124*, 251.

8. Ivanova, J.; Pantcheva, I. N.; Mitewa, M.; Simova, S.; Tanabe, M.; Osakada, K. *Chem. Cent. J.* **2011**, *5*, 52.
9. Riddell, F. G.; Tompsett, S. J. *Tetrahedron* **1991**, *47*, 10109.
10. Pankiewicz, R. *J. Mol. Struct.* **2013**, *1048*, 464.
11. Miyazaki, Y.; Sugawara, H.; Nagatsu, J.; Shibuya, M.; Kaken Chemical Co., Ltd. . 1972, p. 5.
12. Butaye, P.; Devriese, L. A.; Haesebrouck, F. *Clin. Microbiol. Rev.* **2003**, *16*, 175.
13. Mitani, M.; Yamanishi, T.; Miyazaki, Y. *Biochem. Biophys. Res. Commun.* **1975**, *66*, 1231.
14. Mitani, M.; Yamanishi, T.; Miyazaki, Y.; Otake, N. *Antimicrob. Agents Chemother.* **1976**, *9*, 655.
15. Gupta, P. B.; Onder, T. T.; Jiang, G. Z.; Tao, K.; Kuperwasser, C.; Weinberg, R. A.; Lander, E. S. *Cell* **2009**, *138*, 645.
16. Naujokat, C.; Steinhart, R. *J. Biomed. Biotechnol.* **2012**, *2012*, 950658.
17. Tang, Q. L.; Zhao, Z. Q.; Li, J. C.; Liang, Y.; Yin, J. Q.; Zou, C. Y.; Xie, X. B.; Zeng, Y. X.; Shen, J. N.; Kang, T. B.; Wang, J. *Cancer Lett.* **2011**, *311*, 113.
18. Boehmerle, W.; Endres, M. *Cell Death Dis.* **2011**, *2*, e168.
19. Aleman, M.; Magdesian, K. G.; Peterson, T. S.; Galey, F. D. *J. Am. Vet. Med. Assoc.* **2007**, *230*, 1822.
20. Novilla, M. N.; Owen, N. V.; Todd, G. C. *Vet. Hum. Toxicol.* **1994**, *36*, 318.
21. Plumlee, K. H.; Johnson, B.; Galey, F. D. *J. Vet. Diagn. Invest.* **1995**, *7*, 419.
22. Story, P.; Doube, A. *N. Z. Med. J.* **2004**, *117*, U799.
23. van der Linde-Sipman, J. S.; van den Ingh, T. S. G. A. M.; van Nes, J. J.; Verhagen, H.; Kersten, J. G. T. M.; Beynen, A. C.; Plekkringa, R. *Vet. Pathol.* **1999**, *36*, 152.
24. Dittmar, T.; Zänker, K. S. *Role of cancer stem cells in cancer biology and therapy*; Taylor & Francis: Boca Raton, 2013.
25. Kishi, Y.; Hatakeyama, S.; Lewis, M. D. In *Frontiers of Chemistry*; Laidler, K. J., Ed.; Pergamon: 1982, p. 287.
26. Horita, K.; Nagato, S.; Oikawa, Y.; Yonemitsu, O. *Chem. Pharm. Bull.* **1989**, *37*, 1726.
27. Horita, K.; Nagato, S.; Oikawa, Y.; Yonemitsu, O. *Chem. Pharm. Bull.* **1989**, *37*, 1705.
28. Horita, K.; Oikawa, Y.; Nagato, S.; Yonemitsu, O. *Chem. Pharm. Bull.* **1989**, *37*, 1717.
29. Horita, K.; Oikawa, Y.; Yonemitsu, O. *Chem. Pharm. Bull.* **1989**, *37*, 1698.
30. Brown, R. C. D.; Kocienski, P. J. *Synlett* **1994**, 417.
31. Brown, R. C. D.; Kocienski, P. J. *Synlett* **1994**, 415.
32. Kocienski, P. J.; Brown, R. C. D.; Pommier, A.; Procter, M.; Schmidt, B. *J. Chem. Soc.; Perkin Trans. I* **1998**, 9.
33. Brimble, M. A.; Farès, F. A. *Tetrahedron* **1999**, *55*, 7661.
34. Faul, M. M.; Huff, B. E. *Chem. Rev.* **2000**, *100*, 2407.
35. Larrosa, I.; Romea, P.; Urpi, R. *Org. Lett.* **2006**, *8*, 527.
36. Yadav, J. S.; Singh, V. K.; Srihari, P. *Org. Lett.* **2014**, *16*, 836.
37. Solsona, J. G.; Nebot, J.; Romea, P.; Urpi, F. *J. Org. Chem.* **2005**, *70*, 6533.
38. Brimble, M. A. *Molecules* **2004**, *9*, 394.
39. Sperry, J.; Liu, Y. C.; Brimble, M. A. *Org. Biomol. Chem.* **2010**, *8*, 29.
40. Montagnon, T.; Kalaitzakis, D.; Triantafyllakis, M.; Stratakis, M.; Vassilikogiannakis, G. *Chem. Commun. (Camb.)* **2014**, *50*, 15480.
41. Montagnon, T.; Tofi, M.; Vassilikogiannakis, G. *Acc. Chem. Res.* **2008**, *41*, 1001.
42. Tofi, M.; Montagnon, T.; Georgiou, T.; Vassilikogiannakis, G. *Org. Biomol. Chem.* **2007**, *5*, 772.
43. Greenberg, A.; Breneman, C. M.; Liebman, J. F. *The amide linkage: selected structural aspects in chemistry, biochemistry, and materials science*; Wiley-Interscience: New York, 2000.

44. Valeur, E.; Bradley, M. *Chem. Soc. Rev.* **2009**, *38*, 606.
45. Huczynski, A.; Janczak, J.; Stefanska, J.; Antoszczak, M.; Brzezinski, B. *Bioorg. Med. Chem. Lett.* **2012**, *22*, 4697.
46. Pedersen, D. S.; Rosenbohm, C. *Synthesis-Stuttgart* **2001**, 2431.
47. Antoszczak, M.; Maj, E.; Stefanska, J.; Wietrzyk, J.; Janczak, J.; Brzezinski, B.; Huczynski, A. *Bioorg. Med. Chem. Lett.* **2014**, *24*, 1724.
48. Huczynski, A.; Janczak, J.; Antoszczak, M.; Wietrzyk, J.; Maj, E.; Brzezinski, B. *Bioorg. Med. Chem. Lett.* **2012**, *22*, 7146.
49. Stefanska, J.; Antoszczak, M.; Stepień, K.; Bartoszcze, M.; Mirski, T.; Huczynski, A. *Bioorg. Med. Chem. Lett.* **2015**, *25*, 2082.
50. Antoszczak, M.; Maj, E.; Napiorkowska, A.; Stefanska, J.; Augustynowicz-Kopec, E.; Wietrzyk, J.; Janczak, J.; Brzezinski, B.; Huczynski, A. *Molecules* **2014**, *19*, 19435.
51. Antoszczak, M.; Sobusiak, M.; Maj, E.; Wietrzyk, J.; Huczynski, A. *Bioorg. Med. Chem. Lett.* **2015**, *25*, 3511.
52. Huczynski, A.; Janczak, J.; Antoszczak, M.; Stefanska, J.; Brzezinski, B. *J. Mol. Struct.* **2012**, *1022*, 197.
53. Miyazaki, Y.; Kinashi, H.; Otake, N.; Mitani, M.; Yamanishi, T. *Agric. Biol. Chem.* **1976**, *40*, 1633.
54. Antoszczak, M.; Popiel, K.; Stefanska, J.; Wietrzyk, J.; Maj, E.; Janczak, J.; Michalska, G.; Brzezinski, B.; Huczynski, A. *Eur. J. Med. Chem.* **2014**, *76*, 435.
55. Borgstrom, B.; Huang, X. L.; Posta, M.; Hegardt, C.; Oredsson, S.; Strand, D. *Chem. Commun. (Camb.)* **2013**, *49*, 9944.
56. Tulla-Puche, J.; Torres, A.; Calvo, P.; Royo, M.; Albericio, F. *Bioconjug. Chem.* **2008**, *19*, 1968.
57. Hammann, P.; Raether, W.; Vertesy, L. *J. Antibiot. (Tokyo)* **1993**, *46*, 523.
58. Yurkovich, M. E.; Tyrakis, P. A.; Hong, H.; Sun, Y. H.; Samborsky, M.; Kamiya, K.; Leadlay, P. F. *ChemBioChem* **2012**, *13*, 66.
59. Miyazaki, Y.; Shibata, A.; Tsuda, K.; Kinashi, H.; Otake, N. *Agric. Biol. Chem.* **1978**, *42*, 2129.
60. Huang, X. L.; Borgstrom, B.; Mansson, L.; Persson, L.; Oredsson, S.; Hegardt, C.; Strand, D. *ACS Chem. Biol.* **2014**, *9*, 1587.
61. Gazak, R.; Purchartova, K.; Marhol, P.; Zivna, L.; Sedmera, P.; Valentova, K.; Kato, N.; Matsumura, H.; Kaihatsu, K.; Kren, V. *Eur. J. Med. Chem.* **2010**, *45*, 1059.
62. Huczynski, A.; Antoszczak, M.; Kleczewska, N.; Lewandowska, M.; Maj, E.; Stefanska, J.; Wietrzyk, J.; Janczak, J.; Celewicz, L. *Eur. J. Med. Chem.* **2015**, *93*, 33.
63. Skiera, I.; Antoszczak, M.; Trynda, J.; Wietrzyk, J.; Boratynski, P.; Kacprzak, K.; Huczynski, A. *Chem. Biol. Drug Des.* **2015**, *86*, 911.
64. Ivanova, J.; Pantcheva, I. N.; Zhorova, R.; Momekov, G.; Simova, S.; Stoyanova, R.; Zhecheva, E.; Ivanova, S.; Mitewa, M. *J. Chem. Chem. Eng.* **2012**, *6*, 551.
65. Vögtle, F. *Host guest complex chemistry II*; Springer-Verlag: Berlin ; New York, 1982.
66. Huczynski, A. *Bioorg. Med. Chem. Lett.* **2012**, *22*, 7002.
67. Matsumori, N.; Morooka, A.; Murata, M. *J. Am. Chem. Soc.* **2007**, *129*, 14989.
68. Fuchs, D.; Heinold, A.; Opelz, G.; Daniel, V.; Naujokat, C. *Biochem. Biophys. Res. Commun.* **2009**, *390*, 743.
69. Arafat, K.; Iratni, R.; Takahashi, T.; Parekh, K.; Al Dhaheri, Y.; Adrian, T. E.; Attoub, S. *PLoS One* **2013**, *8*, e66931.
70. Antoszczak, M.; Huczynski, A. *Anticancer Agents Med. Chem.* **2015**, *15*, 575.
71. Kim, J. H.; Yoo, H. I.; Kang, H. S.; Ro, J.; Yoon, S. *Biochem. Biophys. Res. Commun.* **2012**, *418*, 98.

72. Parajuli, B.; Lee, H. G.; Kwon, S. H.; Cha, S. D.; Shin, S. J.; Lee, G. H.; Bae, I.; Cho, C. H. *Cancer Epidemiol.* **2013**, *37*, 512.
73. Kim, W. K.; Kim, J. H.; Yoon, K.; Kim, S.; Ro, J.; Kang, H. S.; Yoon, S. *Invest. New Drugs* **2012**, *30*, 1311.
74. Calzolari, A.; Saulle, E.; De Angelis, M. L.; Pasquini, L.; Boe, A.; Pelacchi, F.; Ricci-Vitiani, L.; Baiocchi, M.; Testa, U. *PLoS One* **2014**, *9*.
75. Wang, F.; Dai, W.; Wang, Y.; Shen, M.; Chen, K.; Cheng, P.; Zhang, Y.; Wang, C.; Li, J.; Zheng, Y.; Lu, J.; Yang, J.; Zhu, R.; Zhang, H.; Zhou, Y.; Xu, L.; Guo, C. *PLoS One* **2014**, *9*, e97414.
76. Zhou, J.; Li, P.; Xue, X.; He, S.; Kuang, Y.; Zhao, H.; Chen, S.; Zhi, Q.; Guo, X. *Toxicol. Lett.* **2013**, *222*, 139.
77. Zhang, G. N.; Liang, Y.; Zhou, L. J.; Chen, S. P.; Chen, G.; Zhang, T. P.; Kang, T. B.; Zhao, Y. P. *Cancer Lett.* **2011**, *313*, 137.
78. Lu, W.; Li, Y. *J. Cell. Biochem.* **2014**, *115*, 1799.
79. Lu, D. S.; Choi, M. Y.; Yu, J.; Castro, J. E.; Kipps, T. J.; Carson, D. A. *Proc. Natl. Acad. Sci. U. S. A.* **2011**, *108*, 13253.
80. Fuchs, D.; Daniel, V.; Sadeghi, M.; Opelz, G.; Naujokat, C. *Biochem. Biophys. Res. Commun.* **2010**, *394*, 1098.
81. Jangamreddy, J. R.; Ghavami, S.; Grabarek, J.; Kratz, G.; Wiechec, E.; Fredriksson, B. A.; Pariti, R. K. R.; Cieslar-Pobuda, A.; Panigrahi, S.; Los, M. J. *BBA-Mol. Cell Res.* **2013**, *1833*, 2057.
82. Verdoodt, B.; Vogt, M.; Schmitz, I.; Liffers, S. T.; Tannapfel, A.; Mirmohammadsadegh, A. *PLoS One* **2012**, *7*, e44132.
83. Klose, J.; Stankov, M. V.; Kleine, M.; Ramackers, W.; Panayotova-Dimitrova, D.; Jager, M. D.; Klempnauer, J.; Winkler, M.; Bektas, H.; Behrens, G. M.; Vondran, F. W. *PLoS One* **2014**, *9*, e95970.
84. Al Dhaheri, Y.; Attoub, S.; Arafat, K.; AbuQamar, S.; Eid, A.; Al Faresi, N.; Iratni, R. *BBA-Gen. Subjects* **2013**, *1830*, 3121.
85. Lieke, T.; Ramackers, W.; Bergmann, S.; Klempnauer, J.; Winkler, M.; Klose, J. *BMC Cancer* **2012**, *12*.
86. Kim, J.-H.; Chae, M.; Kim, W. K.; Kim, Y.-J.; Kang, H. S.; Kim, H. S.; Yoon, S. *Br. J. Pharmacol.* **2011**, *162*, 773.
87. Wang, F.; He, L.; Dai, W. Q.; Xu, Y. P.; Wu, D.; Lin, C. L.; Wu, S. M.; Cheng, P.; Zhang, Y.; Shen, M.; Wang, C. F.; Lu, J.; Zhou, Y. Q.; Xu, X. F.; Xu, L.; Guo, C. Y. *PLoS One* **2012**, *7*, e50638.
88. Wu, D.; Zhang, Y.; Huang, J.; Fan, Z.; Shi, F.; Wang, S. *Biochem. Biophys. Res. Commun.* **2014**, *443*, 712.
89. Zhu, L. Q.; Zhen, Y. F.; Zhang, Y.; Guo, Z. X.; Dai, J.; Wang, X. D. *PLoS One* **2013**, *8*, e84175.
90. Koo, K. H.; Kim, H.; Bae, Y. K.; Kim, K.; Park, B. K.; Lee, C. H.; Kim, Y. N. *Cell Death Dis.* **2013**, *4*, e693.
91. Zhang, B.; Wang, X. Y.; Cai, F. F.; Chen, W. J.; Loesch, U.; Bitzer, J.; Zhong, X. Y. *Tumor Biol.* **2012**, *33*, 1855.
92. Riccioni, R.; Dupuis, M. L.; Bernabei, M.; Petrucci, E.; Pasquini, L.; Mariani, G.; Cianfriglia, M.; Testa, U. *Blood Cells Mol. Dis.* **2010**, *45*, 86.
93. Ketola, K.; Hilvo, M.; Hyotylainen, T.; Vuoristo, A.; Ruskeepaa, A. L.; Oresic, M.; Kallioniemi, O.; Iljin, K. *Br. J. Cancer* **2012**, *106*, 99.
94. Kim, K. Y.; Yu, S. N.; Lee, S. Y.; Chun, S. S.; Choi, Y. L.; Park, Y. M.; Song, C. S.; Chatterjee, B.; Ahn, S. C. *Biochem. Biophys. Res. Commun.* **2011**, *413*, 80.

95. An, H.; Kim, J. Y.; Lee, N.; Cho, Y.; Oh, E.; Seo, J. H. *Biochem. Biophys. Res. Commun.* **2015**, *466*, 696.
96. Kusunoki, S.; Kato, K.; Tabu, K.; Inagaki, T.; Okabe, H.; Kaneda, H.; Suga, S.; Terao, Y.; Taga, T.; Takeda, S. *Gynecol. Oncol.* **2013**, *129*, 598.
97. Zhang, B.; Wang, X. Y.; Cai, F. F.; Chen, W. J.; Loesch, U.; Zhong, X. Y. *Oncol. Rep.* **2013**, *29*, 1371.
98. Kevin, D. A.; Meujo, D. A. F.; Hamann, M. T. *Expert Opin. Drug Discov.* **2009**, *4*, 109.
99. Liu, H.; Huang, J.; Peng, J.; Wu, X.; Zhang, Y.; Zhu, W.; Guo, L. *Mol. Cancer* **2015**, *14*, 1.
100. Manago, A.; Leanza, L.; Carraretto, L.; Sassi, N.; Grancara, S.; Quintana-Cabrera, R.; Trimarco, V.; Toninello, A.; Scorrano, L.; Trentin, L.; Semenzato, G.; Gulbins, E.; Zoratti, M.; Szabo, I. *Cell Death Dis.* **2015**, *6*, e1930.
101. Reya, T.; Morrison, S. J.; Clarke, M. F.; Weissman, I. L. *Nature* **2001**, *414*, 105.
102. Khan, I. N.; Al-Karim, S.; Bora, R. S.; Chaudhary, A. G.; Saini, K. S. *Drug Discov. Today* **2015**, *20*, 1205.
103. Zhou, S.; Wang, F. F.; Wong, E. T.; Fonkem, E.; Hsieh, T. C.; Wu, J. M.; Wu, E. X. *Curr. Med. Chem.* **2013**, *20*, 4095.
104. Huczyński, A. *Chem. Biol. Drug Des.* **2012**, *79*, 235.
105. Antoszczak, M.; Klejborowska, G.; Kruszyk, M.; Maj, E.; Wietrzyk, J.; Huczynski, A. *Chem. Biol. Drug Des.* **2015**.
106. Huczyński, A.; Janczak, J.; Lowicki, D.; Brzezinski, B. *BBA-Biomembranes* **2012**, *1818*, 2108.
107. Warburg, O. *Science* **1956**, *123*, 309.